Engineering Functional Nanomaterials Through the Amino Group

Giacomo Filippini[1], Paolo Pengo[1], Susanna Bosi[1], Giulio Ragazzon[1], Lucia Pasquato[1] and Maurizio Prato[1,2,3]

[1] Università degli Studi di Trieste, Dipartimento di Scienze Chimiche e Farmaceutiche, via L. Giorgieri 1, 34127 Trieste, Italy
[2] Center for Cooperative Research in Biomaterials (CIC biomaGUNE), Carbon Bionanotechnology Laboratory, CIC biomaGUNE, Paseo Miramòn, 182, 20014 Donostia San Sebastiàn, Guipuzcoa, Spain
[3] Ikerbasque Basque Foundation for Science, Maria Diaz de Haro 3, 6 Solairua 48013, Bilbao, Spain

Abbreviations

AFG	amino-functionalized graphene
AFM	atomic force microscopy
APTS	(aminopropyl)-triethoxysilane
ATR-IR	attenuated total reflectance infrared
BOC	*t*-butyl carbamate
CDs	carbon dots
CND	carbon nanodiamond
CNHs	carbon nanohorns
CNOs	carbon nano-onions
CNT	carbon nanotube
CPT	camptothecin
CVD	chemical vapor deposition
CVD-G	chemical vapor deposition graphene
DFT	density functional theory
DMAP	4-(dimethylamino)pyridine
DMF	dimethylformamide
DNA	deoxyribonucleic acid
Dod	dodecylamine
ECD	electronical circular dichroism
ECL	electrochemiluminescence
EDC	*N*-ethyl-*N*′-(3-(dimethylamino)propyl) carbodiimide hydrochloride
EGFP	enhanced green fluorescent protein

ESR	electron spin resonance
FITC	fluorescein isothiocyanate
FLG	few layers graphene
f-SWCNT	functionalized single-walled carbon nanotube
GO	graphene oxide
HIV	human immunodeficiency viruses
HoBt	1-hydroxy benzotriazole
HRTEM	high-resolution transmission electron microscopy
IPCA	5-oxo-1,2,3,5-tetrahydroimidazo[1,2-α]pyridine-7-carboxylic acid
IR	infrared
KT	Kaiser test
MPS	3-mercaptopropyltrimethoxysilane
MW	microwave
MWCNHs	multiwalled carbon nanohorns
MWCNT	multiwalled carbon nanotube
NCD	nitrogen-doped carbon dot
ND	nanodiamonds
NMP	*N*-methylpyrrolidone
NMR	nuclear magnetic resonance
NP	nanoparticle
NR	nanorods
NTA	nitrilotriacetic acid
Oct	octylamine
ODE	1-octadecene
OEAs	oxygen evolving anodes
OLE	oleylamine
ORR	oxygen reduction reaction
OTS	octadecyltrichlorosilane
PAMAM	poly(amidoamine)
PC	prostate cancer
PEG	polyethylene glycol
PEI	polyethyleneimine
PLQY	photoluminescence quantum yield
POM	polyoxometalate
PSMA	prostate-specific membrane antigen
PVP	polyvinylpyrrolidone
QDs	quantum dots
SAM	self-assembled monolayers
SCE	saturated calomel electrode
siRNA	small-interfering ribonucleic acid
SP	supraparticle
SWCNHs	single-walled carbon nanohorns
SWCNT	single-walled carbon nanotube
SWNT	single-walled nanotube
TEM	transmission electron microscopy

TFA	trifluoroacetic acid
TGA	thermogravimetric analysis
TIPS	triisopropylsilane
TLC	thin-layer chromatography
TMEDA	tetramethylethylendiamine
TOP	tri-*n*-octylphosphine
TOPO	tri-*n*-octylphosphine oxide
VCD	vibrational circular dichroism
XPS	X-ray photoelectron spectroscopy

8.1 Introduction

In the past two decades, the fast scientific and practical evolution of nanomaterials has led to applications that can improve our everyday life. The design, preparation, characterization, and study of nanomaterial properties and features are now moving toward a convergence of technologies developed in different fields such as nanotechnology, biotechnology, information technology, and cognitive sciences. The evolution so far observed and the new outcome are guided by the heavy work of scientists, who develop (nano)materials with new properties, proposing environmentally sustainable procedures for their preparation, introducing innovation for reproducible and large-scale production.

Chemistry and in particular organic chemistry offers a variety of tools to design, synthetize, or assemble building blocks combining organic and inorganic materials for the construction of architectures with nanometer dimension, functional nanomaterials, and integrate biomaterials with nanomaterials. Moreover, organic chemistry enables an infinite variety in the design of electronic, optical, and catalytic properties of (nano)materials.

In this context, the chemistry of the amino group is of paramount importance. Indeed, amines have been widely employed to design and produce a large variety of novel smart nanomaterials addressing many of the targets for innovation and sustainability.

In particular, in this chapter, we describe and analyze the most common strategies that use amines in nanomaterial preparation or that enable efficient ways for introducing amino groups in nanomaterials for further functionalization.

To this end, we selected two main types of nanomaterials, which have become very popular in the past decades: carbon-based nanomaterials and hybrid organic–inorganic nanoparticles (NPs), which are our main research fields. In particular, we mainly focus on fullerenes, carbon nanotubes (CNTs), graphene, and on less common carbon nanomaterials, namely, carbon nano-onions (CNOs) and nanodiamonds (NDs). We also take into consideration the emerging members of this family, i.e. carbon nanodots. Then, we present the use of amines in the synthesis, stabilization, and functionalization of organic–inorganic hybrid nanomaterials, such as two dimensional self-assembled monolayers (2D SAMs), semiconductor quantum dots (QDs), and metal or metal oxide nanoparticles. These apparently very different types of materials heavily rely on similar wet chemistry approaches for their preparation, stabilization, functionalization, and processing. These are rooted down to very fundamental properties of amines such as their Lewis basicity, nucleophilic character, and hydrogen bond acceptor ability. Beside their role in the synthesis or modification of the

materials, amines are also keys to unlock numerous practical nanomaterial applications in the fields of biology, medicine, sensor development, and energy production. Some proof-of-principle examples are briefly discussed to further highlight the scope of amines in producing novel ad hoc nanomaterials and how amines can affect and address their final applications.

8.2 Quantification of Nanomaterial-Bound Amino Groups

In an overview of the amino group in nanomaterials, it seems adequate to recall how amino groups can be identified and quantified. Several possible strategies have been used, and often, they can be considered complementary with one another. Here, we recall those which have been most commonly used in the analysis of nanomaterials.

Ideally, spectroscopic techniques that do not require chemical reactivity of the amino group are preferred (Figure 8.1a). However, gaining direct spectroscopic evidence of the presence of amino groups may not be straightforward. Nuclear magnetic resonance (NMR) techniques are certainly very powerful. Simple ^{1}H-NMR can be used if the amine structure is known because the protons of the amino group may not be very diagnostic. However, solution NMR techniques often suffer from the limited mobility of molecular fragments attached to the nanomaterial [3]. ^{15}N-NMR has also been used for this purpose, having the evident advantage of detecting directly the N-nucleus [4]. However, this technique requires the use of ^{15}N-labeled compounds, which is often not practical. X-ray photoelectron spectroscopy (XPS), infrared (IR) spectroscopy, and thermogravimetric analysis (TGA) – among others – can provide qualitative evidence in support of other employed strategies [5]. In some cases, XPS can be particularly useful, although it has two important limitations that should be recalled. The first limitation is that, as it detects the core of the nitrogen atom, in the presence of several types of nitrogen atoms in the nanomaterial, the technique may not be sufficiently selective to identify amino groups. To some extent, the multicomponent fitting of the acquired nitrogen peak data can limit this shortcoming, albeit not completely. The second limitation is that it is a surface technique; therefore, it is inappropriate to test bulk materials, albeit this can also be a strength when the surface properties of the nanomaterial are of particular interest.

A different class of strategies rely on the detection of amino groups exploiting its reactivity. Intrinsically, these methods are strongly dependent on the type of amine to be determined. In the simplest case, acid–base titrations can be used for the quantification [6]. Absorption measurements can also be used, e.g. upon interaction with suitable dyes, and also as fluorogenic precursors such as fluorescamine [7].

In many cases, the chemical detection of amines relies on the formation of imine derivatives (Figure 8.1b). Examples of reaction partners suitable for NMR quantification are 4-nitrobenzaldehyde and 3,5-bistrifluoromethyl-benzaldehyde, which were used for spectrophotometric or ^{19}F-NMR detection, respectively [1]. One of the most widely used tests for the identification of amines is the reaction with ninhydrin, affording a colored product. This colorimetric analysis is based on the same principle of the commonly used thin-layer chromatography (TLC) stain. In particular, a variant of the ninhydrin reaction, performed under basic conditions in the presence of KCN, is known as the Kaiser test (KT),

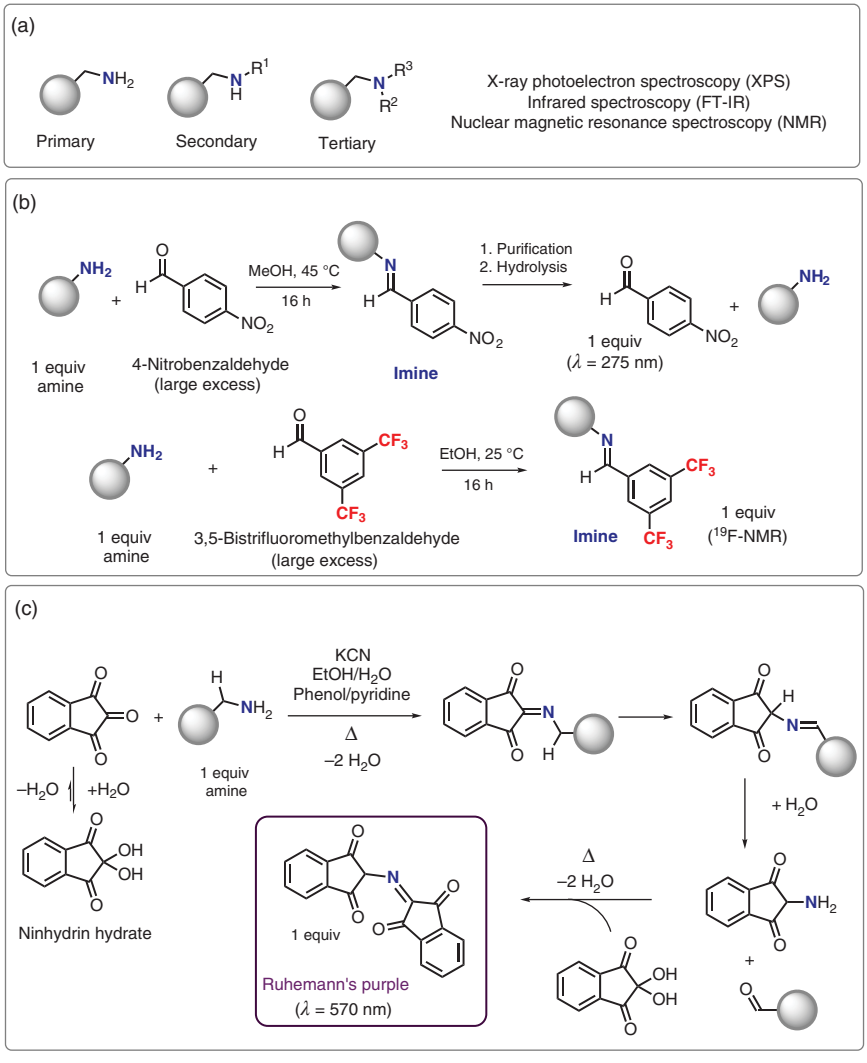

Figure 8.1 Overview of the various methods to identify and quantify amino groups present on nanomaterials. (a) Prominent spectroscopic techniques employed for the detection of primary, secondary, and tertiary amines. (b) Strategies based on imine formation with aromatic aldehydes, for the identification of primary amines. Source: Based on Sun et al. [1]. (c) Reaction sequence associated with the Kaiser test that can disclose primary aliphatic amines having one proton attached to the α−carbon. Source: Based on Sarin et al. [2c].

that is commonly employed for the quantitative identification of amines, especially during peptide synthesis (Figure 8.1c) [2]. This colorimetric test has also been applied for amines on nanomaterials, including CNTs, nanoparticles, and surfaces [8]. In the past decades, we had the opportunity to appreciate the simplicity of the Kaiser test that has been frequently used in our laboratories to test different amino-functionalized nanomaterials.

Importantly, the Kaiser test is selective for the detection of primary amines, with at least one proton on the α carbon atom. Following imine formation, a multistep mechanism affords a colored product known as Ruhemann's purple. Importantly, the molecular structure of this intensely colored product is independent on the starting amine, allowing a reliable colorimetric quantification.

It should be noted, however, that not all primary amines afford a quantitative test, as evidenced by studies performed to optimize the test conditions. Moreover, the colored product suffers from limited stability under the test conditions [2]. For these reasons, the Kaiser test can be considered a quantitative test that however underestimates the total number of amines. This was indeed confirmed by studies on silica matrices rich in amino groups that were tested with different methods for amine detection [1]. Finally, limited accessibility of amino groups has also been described as a possible reason for an incomplete quantification of the reactive groups. Indeed, matrix effects may hamper the reactivity, in particular at a high surface coverage of functional groups.

8.3 Exploiting Amino Compounds for the Functionalization of Carbon-Based Nanomaterials

8.3.1 Historical Backgrounds: Allotropes of Carbon

The discovery of fullerenes as the first molecular allotropes of carbon in 1985 [9] and their further preparation in macroscopic amounts by arc vaporization of graphite in 1990 [10] have profoundly influenced many aspects of contemporary chemistry. Since then, the family of carbon nanoforms has grown significantly, first with the closely related CNTs [11] and, more recently, with the advent of graphene in 2004 [12]. Nowadays, carbon-based nanomaterials are fully recognized as very useful carbon building blocks with potential applications in different scientific fields [13]. In fact, all carbon allotropes may undergo chemical transformation that enhance both their solubility and processability, with the aim of integrating them into inorganic, organic, and biological systems. The reactivity of these nanostructures toward addition reactions was found to be strongly dependent on the curvature of their carbon frameworks and thus on the pyramidalization degrees of their sp^2-hybridized carbon atoms [14]. Elevated pyramidalization levels of the sp^2-hybridized carbon atoms make, typically, the materials more susceptible toward functionalization reactions, and a general reactivity series may be indicated as follows: fullerenes > CNTs > graphene [15]. Moreover, in graphene, which can ideally be considered as a flat polycyclic aromatic hydrocarbon, the sheet edges are generally considered the most reactive sites [16]. This section of the chapter focuses, through the analysis of some explicative examples, on the most common protocols used for the derivatization of carbon-based nanostructures using amino compounds, and on the applications of the resulting functionalized materials.

8.3.2 Use of Amines for the Functionalization of Carbon Nanostructures

Amino compounds have been largely capitalized to covalently functionalize carbon-based nanostructures over recent years. In Figure 8.2a,b, two historical and relevant examples

of this type of chemical processes are shown, the 1,3-dipolar cycloaddition of azomethine ylides and the radical arylation reaction. The former reaction, originally performed on C_{60} (fullerene) is a particular version of the well-known cycloaddition to olefins [20]. The amino group in sarcosine reacts with paraformaldehyde to give an iminium salt, which undergoes fast decarboxylation when heated, thus forming the corresponding azomethine ylide intermediate (**Ia**, Figure 8.2a). This species then reacts with C_{60} via a 1,3-dipolar cycloaddition pathway to afford an *N*-methylpyrrolidine derivative (**1a**) in moderate isolated yield (41%) [17]. Remarkably, a wide variety of fullerene derivatives (**1**) can be easily obtained through the rational choice of the amino acids and carbonyl compounds (aldehydes or ketones), showing both the versatility and robustness of this approach (Figure 8.2a, light blue box) [21]. The cycloaddition of azomethine ylides is still an easy and very general approach, commonly followed nowadays, for the production of fullerene derivatives with the structure of **1**. Other convenient methods for the synthesis of pyrrolidinofullerenes (**1**) are based on the thermal ring opening of aziridines, acid-catalyzed or thermal desilylation of trimethylsilylamino derivatives, or photochemical treatment of tertiary amines with C_{60} [22]. In 2006, the reversibility of the reaction on C_{60} was also demonstrated [23]. Indeed, the thermal cycloelimination of the pyrrolidine moiety within **1** could take place in the presence of a strong dipolarophile, such as maleic anhydride, and a metal complex (e.g. Wilkinson's catalyst or copper triflate), thus regenerating the pristine C_{60} fullerene.

Later in 2009, the first asymmetric metal-catalyzed 1,3-dipolar cycloaddition reaction onto C_{60} fullerene was reported, which gives rise to chiral pyrrolidinofullerenes (**1**) with complete control of the stereochemical outcome [24]. This approach has paved the way to the development of numerous catalytic protocols for the enantioselective functionalization of fullerenes, therefore leading to the production of a wide variety of chiral fullerene derivatives with high site and regioselectivity [25].

These optically active materials have found applications in fields where chirality is a key issue, such as medicinal chemistry and nanobiotechnology [26].

CNTs ideally consist of graphitic sheets, which have been rolled up into a cylindrical shape. The length of CNT is in the size of micrometers with diameters up to 100 nm. CNTs form bundles, which are entangled together in the solid state giving rise to complex networks. Depending on the arrangement of the hexagon rings along the tubular surface, CNTs can be metallic or semiconducting [27].

Because of their extraordinary properties, CNTs can be considered as attractive candidates in diverse nanotechnological applications, such as fillers in polymer matrixes, molecular tanks, (bio)sensors, and many others. Since their discovery in 1991, there has been a great deal of interest in the organic derivatization of single-walled carbon nanotubes (SWCNTs) to facilitate their manipulation, enhance their solubility, and make them more amenable to composite formation [28].

In 2001, Tour and coworkers developed a novel and efficient radical approach for the functionalization of small-diameter (c. 0.7 nm) SWCNTs (**2**) [29] that exploits the reactivity of aryl diazonium salts (Figure 8.2b) [18]. As the diameter of these nanotubes (**2**) is approximately the same as that of C_{60}, they were expected to display enhanced reactivity with respect to larger diameter CNTs. The diazonium salts used to derivatize the pristine SWCNTs (**2**) were freshly prepared from the corresponding aniline derivatives using nitrosonium tetrafluoroborate ($NOBF_4$) at low temperature (−30 °C). The

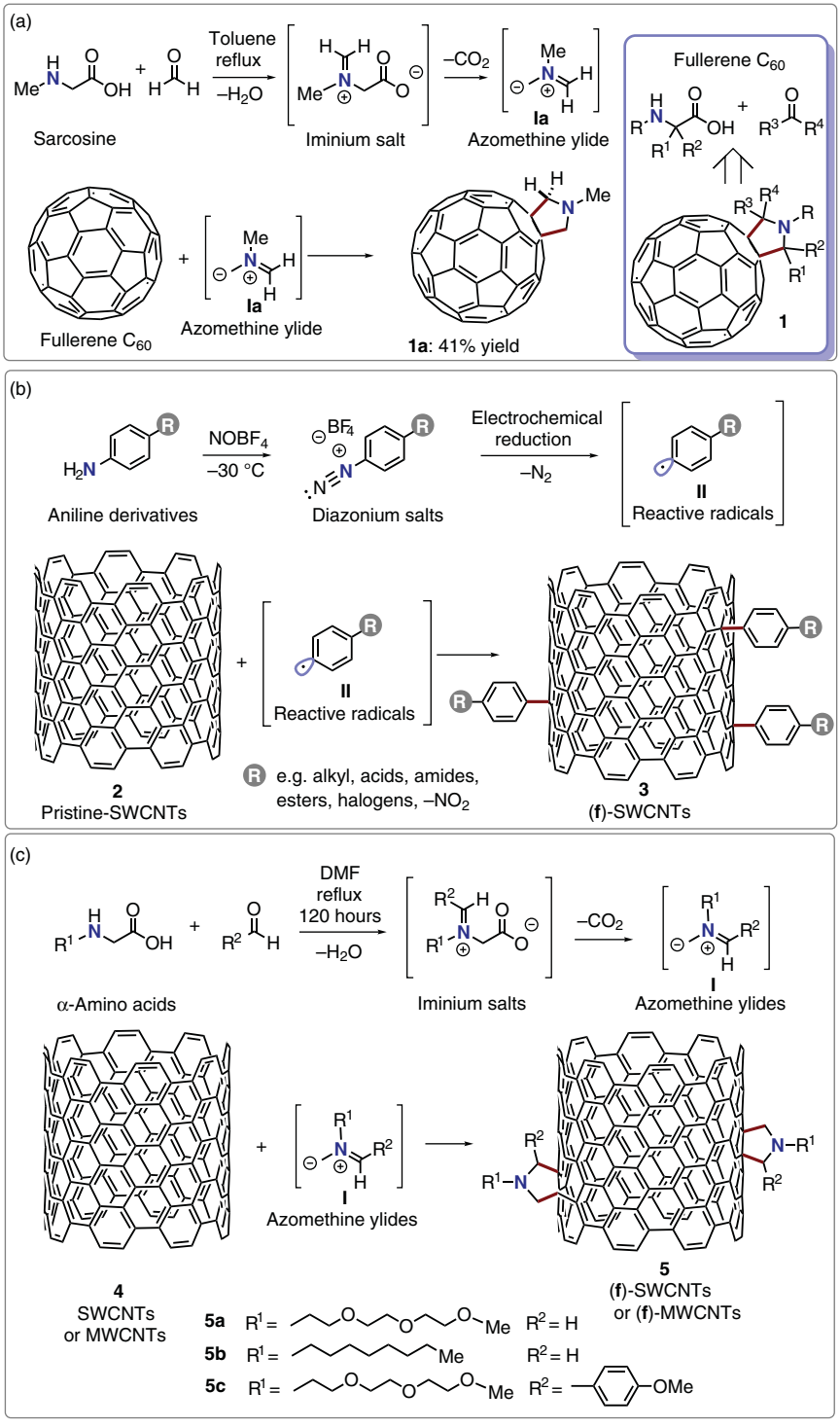

Figure 8.2 (a) Cycloaddition of azomethine ylides to C_{60}. Source: Based on M. Maggini et al. [17]. (b) Arylation reaction on SWCNTs. Source: Based on J. L. Bahr et al. [18]. (c) Cycloaddition of azomethine ylides to CNTs. Source: Based on Georgakilas et al. [19].

subsequent electrochemical reduction of these diazonium salts provided the corresponding reactive aryl radicals (**II**) that covalently bind to the carbon surface, yielding the functionalized single-walled carbon nanotubes (***f***-SWCNTs) (**3**). The functionalization degrees depend on the nature of the para-substituent (–R) within **II** and have been evaluated by combining Raman and TGA. In 2002, a versatile methodology for the organic functionalization of CNTs by using the 1,3-dipolar cycloaddition of azomethine ylides was reported (Figure 8.2c) [19]. The pristine materials (**4**) were suspended in dimethylformamide (DMF), together with an excess aldehyde and the suitable α-amino acid. The heterogeneous reaction mixture was then heated at 130 °C for five days. After workup, the functionalized nanotubes (e.g. **5a–c**) were obtained, which were soluble in chloroform, dichloromethane, acetone, methanol, and ethanol; less soluble in toluene and tetrahydrofuran; and practically insoluble in diethyl ether and hexane. Remarkably, any moiety could be, in principle, attached to the tubular network of CNTs by employing these two derivatization approaches (Figure 8.2b,c) [30]. Moreover, both cycloaddition and arylation reactions, typically, work efficiently with both SWCNTs and multiwalled carbon nanotubes (MWCNTs). The main problem of insolubility of CNTs in aqueous media has been solved by developing a two-step synthetic protocol that allows installing numerous superficial positively charged hydrophilic functionalities at their surfaces (Figure 8.3a). The resultant amino-functionalized CNTs (e.g. **5e–f**) show high aqueous solubility and were particularly suitable for the covalent immobilization of molecules or for further functionalization of the surface based on multiple positive/negative charge interactions (Figure 8.3) [33]. Indeed, various biomolecules have been attached on these amino-CNTs (**5e,f**), such as amino acids, peptides (shown in Figure 8.3b), or nucleic acids [31].

Several applications in the field of medicinal chemistry have been pursued through this approach, including vaccine and drug delivery, gene transfer, and immunopotentiation [34]. Afterward, it was demonstrated that materials of the type of **5e,f** can be subjected to a series of alkylation reactions with glycidyltrimethylammonium chloride, and/or with a mixture of acrylate and ethylenediamine, to obtain a novel family of dendron-functionalized MWCNT derivatives, which are characterized by the presence of numerous positively charged tetra-alkyl ammonium salts at the periphery of the dendrons [35]. These functionalized and charged MWCNTs showed excellent chemical stability and aqueous solubility that increases with the number of the tetra-alkyl ammonium units present at their surfaces and thus with the functionalization degree of the materials (aqueous solubility up to 3 mg/ml). In 2010, the use of these water-soluble dendron MWCNTs for the production of new electrodes suitable for the water-splitting process was exploited (Figure 8.3c) [32]. Indeed, a very efficient and stable nanostructured oxygen-evolving anode can be obtained by the assembly of an oxygen-evolving polyoxometalate (POM) cluster [36], that is, a totally inorganic ruthenium catalyst, with a conducting bed of positively charged dendron MWCNTs. The electrostatic capture of the POMs by the polycationic MWCNTs surface thus allowed for the fabrication of a stable and efficient electrode, which addresses the major challenge of artificial photosynthesis, namely, efficient water oxidation.

Single functionalization protocols of carbon-based nanostructures, namely, C_{60} and CNTs, have been discussed up to this point of the chapter. In addition to single transformations, multiple functionalization reactions represent powerful tools to decorate with more than one functional group of the nanomaterial surfaces (e.g. CNTs) [37]. In 2008, a

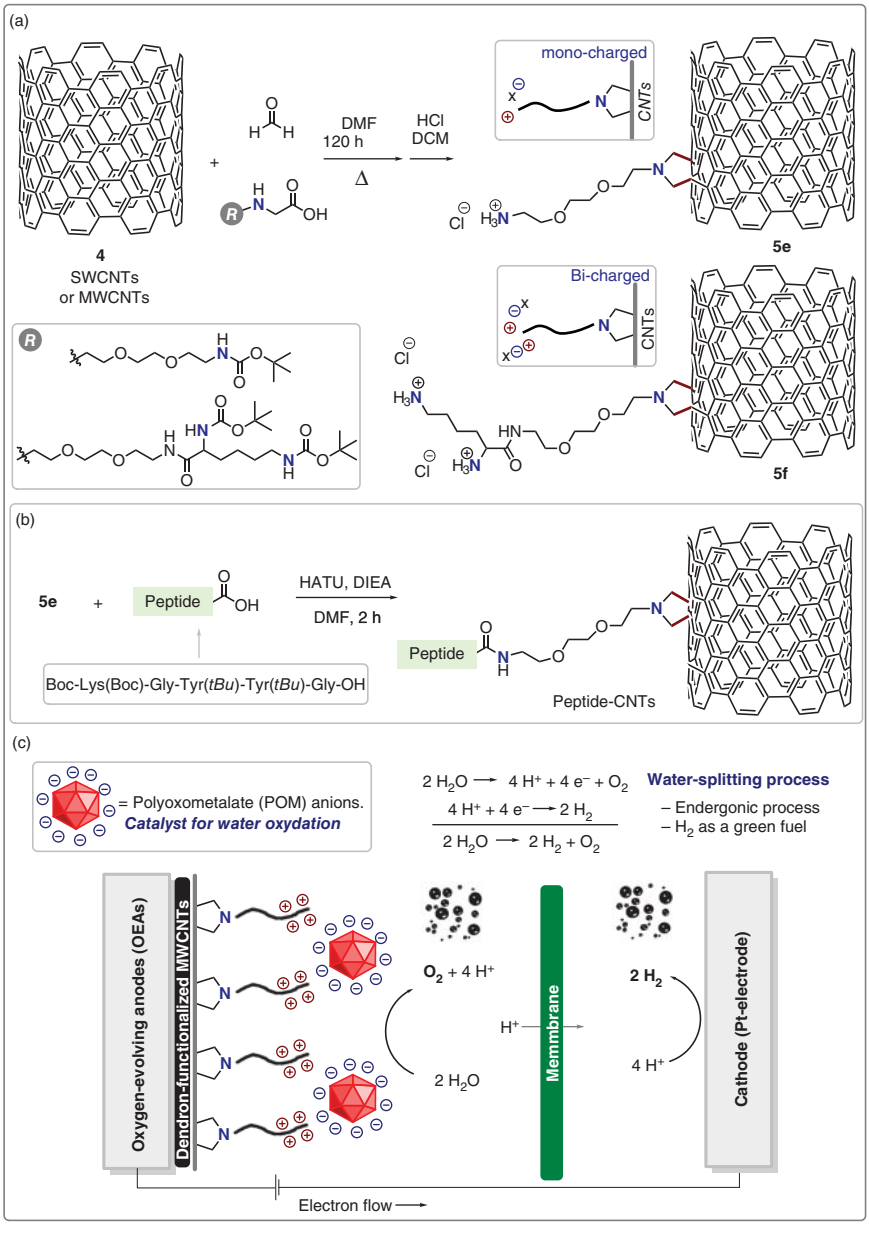

Figure 8.3 (a) Reaction pathway for obtaining water-soluble ammonium-modified nanotubes. (b) Covalent functionalization of superficial amines of CNTs with a biologically active peptide. Source: Based on Pantarotto et al. [31a]. (c) Electrostatic capture of negatively charged polyanionic ruthenium-containing clusters and general scheme for a water-splitting electrocatalytic cell with the integrated nanostructured oxygen evolving anodes (OEAs). Source: Based on Toma et al. [32].

novel, synthetic, two-step strategy to produce multifunctionalized CNTs was described, by employing a combination of two different transformations, the 1,3-dipolar cycloaddition of azomethine ylides (**I**) and the radical addition of diazonium salts, both via a simple and fast microwave (MW)-induced method (Figure 8.4a) [39]. A solvent-free cycloaddition reaction combined with a MW irradiation afforded functionalized nanotubes (**5g–j**) in just one hour. This method significantly improves the productivity of the derivatization process (reaction performed over 120 hours in the primal approach, see Figure 8.2c) and thus paves the way to large-scale functionalization [40]. The resultant materials were then subjected to diazonium salt reaction to introduce other functional groups on the same single-walled nanotubes (SWNTs). Therefore, ***f***-SWNTs (**5g–j**) were dispersed in water with *p*-toluidine and isoamyl nitrite, and this mixture was heated for 90 minutes at 80 °C in a microwave reactor. Mechanistically, the aniline derivative could attack the nitrite group giving the corresponding diazonium and alkoxide species (Figure 8.4a, light blue box). This anionic species (alkoxide) could then add to the electrophilic diazonium salt, thus yielding a diazoether intermediate, which might eventually decompose with release of nitrogen and generation of an aryl radical (**IIa**). This radical could react with the CNT, thus producing **6a–d**. This proposed mechanism is still being discussed at present [38]. In 2011, a novel methodology to covalently functionalized SWCNTs with three different active groups, in one step, by employing the arylation reaction was developed (Figure 8.4b) [8b]. The CNTs (**7a**) are functionalized with numerous benzylamine moieties blocked with three orthogonal protecting groups that can be selectively removed under specific conditions. The sequential removal of the protecting groups of the amine functions might allow for a precisely controlled grafting of molecules of interest onto the nanotube surfaces.

Graphene is a single atomic layer of sp^2-hybridized carbon atoms arranged in a honeycomb lattice with dimensions ranging from a few hundred nanometers to tens of micrometers [41]. Many different types of graphenes can also be defined depending on the number of layers, layer dimension, and amount of oxygen present in the carbon structure [42]. The family of graphene-based materials exhibits a unique set of electronic, mechanical, and thermal properties [43]. Consequently, a wide variety of applications have been designed for graphene materials in sensing, energy storage, catalyst support, supercapacitors, and optoelectronic devices [44]. In most of these applications, graphene is supported on a substrate because the production and handling of graphene in solution is technically challenging. This is due to the metastable nature of graphene and consequently to its tendency toward restacking. The chemical functionalization of single- and few-layer graphene (FLG), both on a support and in solution, is a topic of paramount importance because it allows for the fine-tuning of the materials' chemical and physical properties [45].

The following two examples concern the covalent functionalization of graphene with amines either in solution for the production of a gold-containing nanocomposites or on a substrate to anchor a biologically active protein (Figure 8.5). A mixture of single- and FLG (**8**) can be produced by dispersion and exfoliation of graphite in *N*-methylpyrrolidone (NMP) [47]. The use of this technique allows to effectively produce single- and FLG without the need for intercalants, polymers, or surfactants, which might interfere with the subsequent material manipulations. Functionalized graphene was then prepared by condensation of paraformaldehyde with a modified α-amino acid, followed by the deprotection of the *t*-butyl carbamate (BOC) group to afford **9** (Figure 8.5a) [8f]. To assess

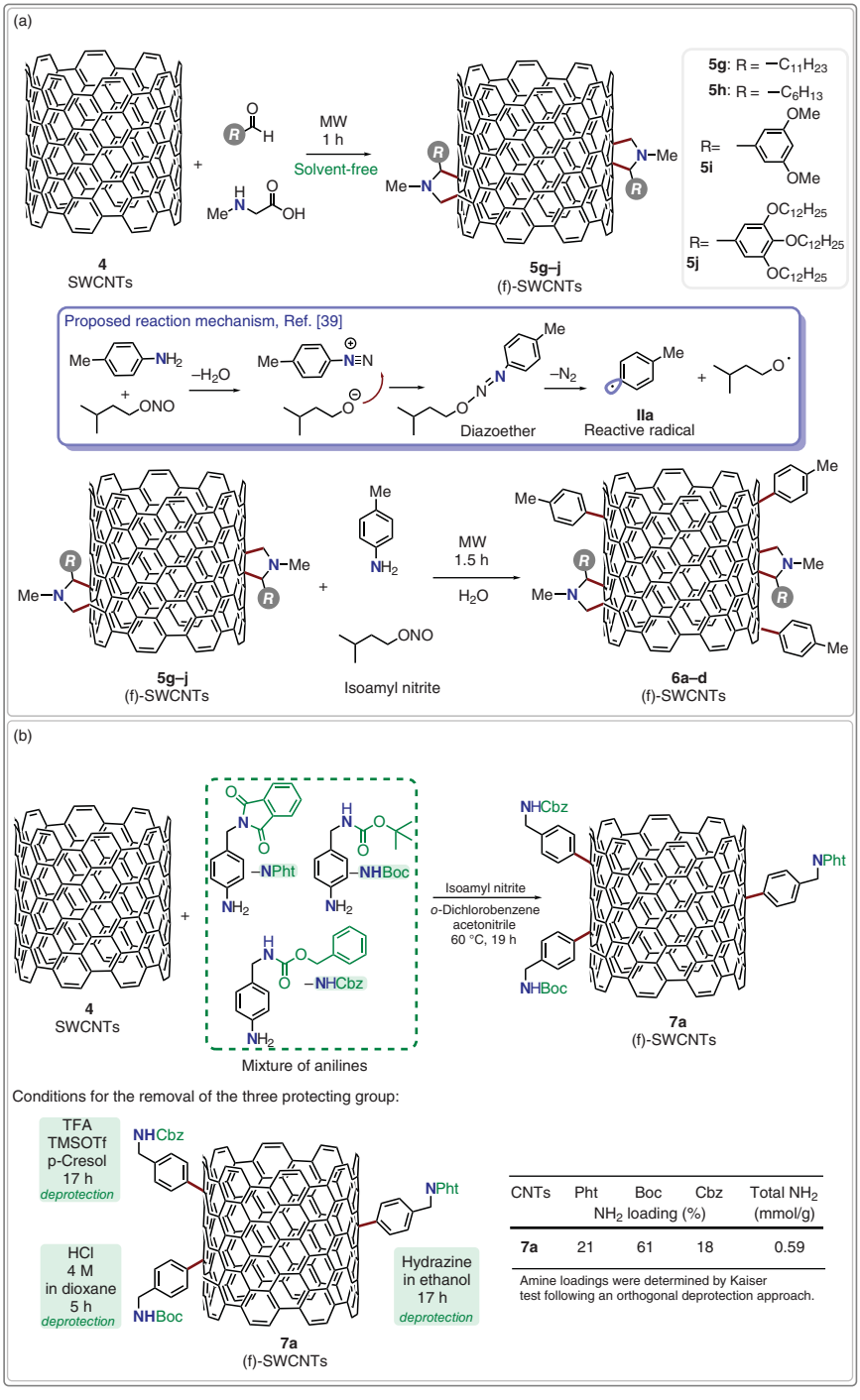

CNTs	Pht	Boc	Cbz	Total NH_2
	NH_2 loading (%)			(mmol/g)
7a	21	61	18	0.59

Amine loadings were determined by Kaiser test following an orthogonal deprotection approach.

Figure 8.4 (a) Synthetic protocol for the MW-induced double functionalization of CNTs. Source: Based on Lipinsk et al. [38]. (b) One-pot triple functionalization of CNTs [39]. Source: Based on Ménard-Moyon et al. [8].

the presence of free amino groups in the resultant product (**9**), the authors performed a quantitative Kaiser test [2c]. The amount of amine functions in **9** was therefore measured to be in the range of 0.64 ± 0.07 mmol/g of material. This is a high value if one takes into account only the functionalization of the edges of graphene sheets, which are considered to be the most reactive sites.

This is an indication that 1,3-dipolar cycloaddition must also take place in the less-reactive central carbon–carbon bonds of graphene layers. The presence of all these superficial amines was utilized for producing a nanocomposite (**10**) with gold nanorods (Au-NRs). The sheets of this hybrid material were characterized by transmission electron microscopy (TEM), which demonstrated the presence of Au-NRs distributed uniformly over the graphene surface. This second observation also confirmed that the reaction took place not just at the edges but also at the internal C—C bonds of graphene.

Another and very popular approach for the functionalization of graphene surfaces is the addition of aryl radicals generated by the reduction of diazonium salts [48]. This strategy, typically, leads to high functionalization degrees and also has the advantage of being tolerant to a variety of conditions (e.g. the solvent used).

The chemical properties of graphene, when it is placed on a substrate, depend strongly on the graphene shape, number of layers, and nature of the substrate. Naturally, this dependence is also reflected in the reactivity with diazonium species [49]. As an example, graphene grown via chemical vapor deposition-graphene (CVD-G) was transferred through reactivity imprint lithography onto a patterned substrate displaying both hydrophobic (OTS, octadecyltrichlorosilane) and hydrophilic (SiO_2) areas (Figure 8.5b) [46]. Then, the supported graphene **11** was functionalized with 4-carboxyphenyldiazonium tetrafluoroborate. The efficient introduction of the carboxyphenyl moieties in **12** has been confirmed by attenuated total reflectance infrared (ATR-IR) analysis. Attachment of these organic units on graphene allowed to establish amide bonds with *N*α,*N*α-bis(carboxymethyl)-L-lysine hydrate, thus leading to the formation of **13** with superficial nitrilotriacetic acid (NTA) units that could be employed to chelate metals. In this way, upon addition of $NiCl_2$, functionalized graphene displayed NTA–Ni complexes that were used as anchors for polyhistidine (His)-tagged enhanced green fluorescent protein (EGFP), allowing for detection of resulting **14** by confocal fluorescence microscopy.

8.3.3 Other Functionalization Procedures of Common Carbon Nanostructures

In this section, we discuss other notable examples related to the derivatization of common carbon-based nanostructures, namely, fullerenes, CNTs, and graphene, which may lead to the formation of various different superficial amino-containing functionalities.

The extraordinary chemical and physical properties of C_{60} and its derivatives might confer activity of these compounds as potential therapeutic agents against human immunodeficiency viruses (HIV) and neurodegenerative diseases and as agents for deoxyribonucleic acid (DNA) cleavage [50].

However, the insolubility of fullerenes in aqueous media has dramatically slowed down the realization of these biological applications. In 2000, the Schuster and Wilson groups reported a methodology for the production of a novel family of amino-substituted methanofullerenes (**15**, $n = 1, 3, 6$), which exhibit pronounced water solubility

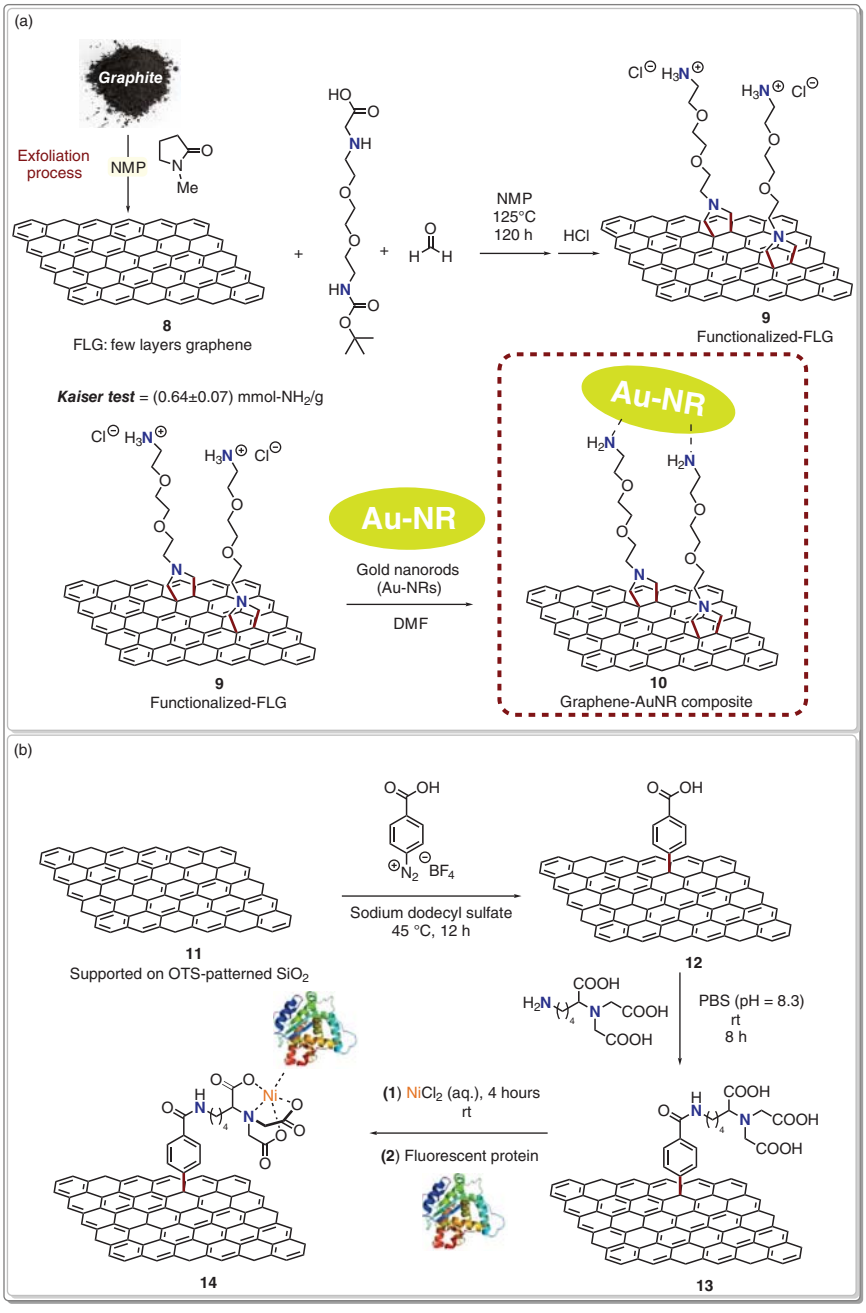

Figure 8.5 (a) Functionalization of graphene via 1,3-dipolar cycloaddition and production of a graphene–Au nanorod composite. Source: Reprinted with permission from Quintana et al. [8]. Copyright 2010, American Chemical Society. (b) Synthetic procedure to anchor a fluorescent protein on graphene . Source: Based on Wang et al. [46].

(Figure 8.6a) [51]. These amino-functionalized fullerenes (**15**) have been obtained through a Bingel–Hirsch [54] reaction between an N-protected malonic derivative and C_{60}, followed by the rapid and effective removal of amine Boc-protecting groups with trifluoroacetic acid (TFA). After the following workup, the crude reaction mixture containing all products **15** was separated on a silica gel column. Interestingly, the exa-amino derivative ($n = 6$), which bears 12 positive charges, showed excellent aqueous solubility (418 mg/ml).

Supercritical fluids (e.g. supercritical carbon dioxide or supercritical water) are regarded as eco-friendly alternatives to organic solvents. There have been many examples of their use in chemical synthesis, usually under homogeneous conditions without the need for other solvents [55]. In contrast to ionic liquids or fluorinated solvents, supercritical fluids represent a different kind of alternative solvent because they are not in the liquid state. In fact, these fluids show low viscosity and no surface tension, and the interactions between solvent molecules and the solute are weak, so high diffusivities are reached, close to those in the gas phase. Recently, supercritical ammonia has been utilized in the chemical modification of MWCNTs (Figure 8.6b) [52]. Such a fluid was able to introduce several amino groups in the pristine nanotubes **16**, giving **17**, while it is more likely that the conversion of carboxylic groups into amides (**19**) took place when oxidized-MWCNTs **18** were used as starting materials.

Recently, it was demonstrated that amino-functionalized graphene (AFG) is a potentially safe material suitable for in vivo biomedical applications [53]. AFG can be produced following the methodology described in Figure 8.6c. Graphene oxide (GO, **20**) sheets can be prepared by refluxing the commercially available graphite powder with a strongly acidic mixture of sulfuric and nitric acid [56]. Material **21** is then obtained by a rapid thermal treatment (1100 °C) of GO (**20**) under argon atmosphere that reduces functional epoxy and hydroxyl groups from the surface of GO-sheets, upon evolution of CO_2, thus leading to the formation of vacancies in the nanostructure. Afterward, the carboxylic acids within **21** are reacted in a mixture of $SOCl_2$ and DMF to produce the corresponding graphene-COCl derivative. This material can be treated first with sodium azide and then with concentrated hydrochloric acid to yield the desired amino-functionalized graphene product (**22**). Subsequently, in 2014, amine-functionalized graphene has also been used as a metal-free catalyst for the oxygen reduction reaction (ORR), a redox process that may produce either water or hydrogen peroxide [57]. The electrochemical results show that AFG is an active catalyst in oxygen reduction reaction and exhibits an electrocatalytic activity much higher than graphene. The significantly high electrochemical performance of AFG could be attributed to its specific structure, which possesses electron-donating groups (e.g. amines), a large number of holes in its sheet plate and the porous structure of the bulk material, arising from the randomly stacked AFG layers.

8.3.4 Exfoliation of Graphite with Melamine

As mentioned above, graphene and its derivatives are novel and extraordinary carbon-based materials expected to revolutionize the electronic industry [58]. Although considerable scientific progress has been achieved in this field of research, the key to commercializing graphene lies in the development of a cost-effective and scalable production method. The biggest problem concerning the exfoliation of graphite is associated with the high energy

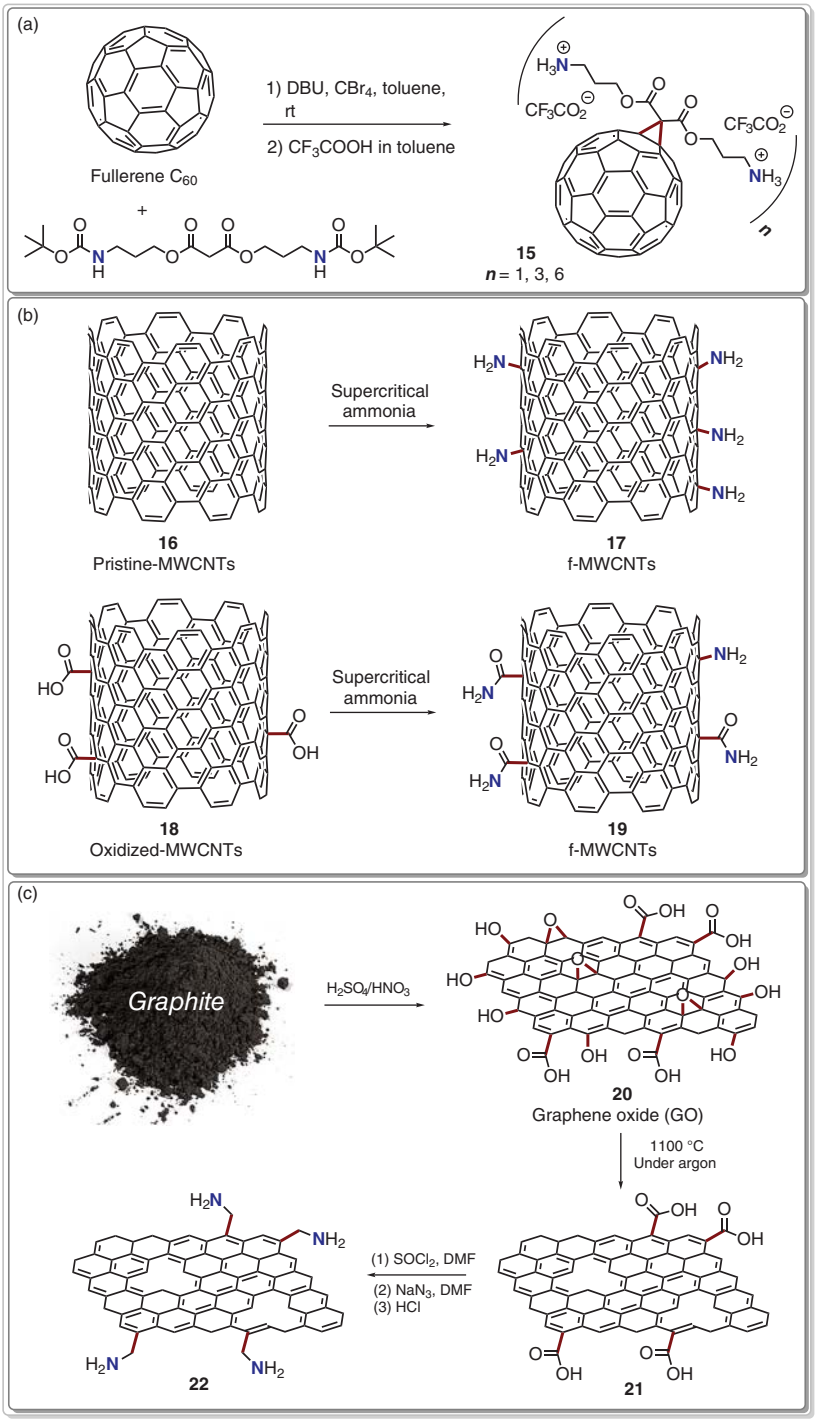

Figure 8.6 (a) Synthetic protocol for the production of water-soluble amino fullerene derivative. Source: Based on Richardson et al. [51]. (b) MWCNTs functionalized with amino groups by the use of supercritical ammonia. Source: Based on Shao et al. [52]. (c) Synthesis of amine-modified graphene. AFG, amino functionalized graphene. Source: Reprinted with permission of Singh et al. 2012 [53]. Copyright 2012, American Chemical Society.

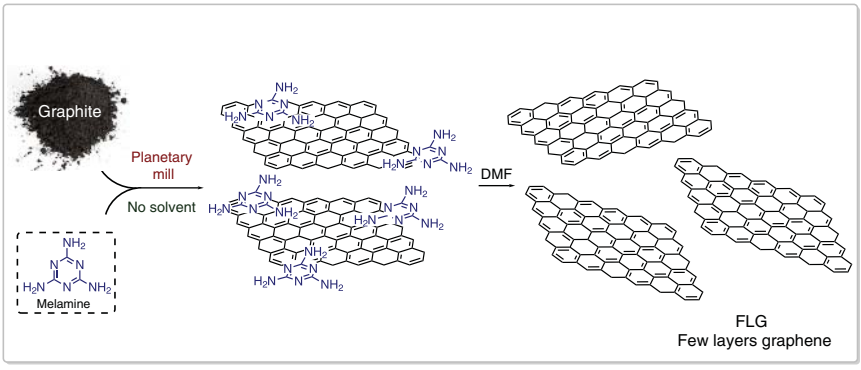

Figure 8.7 Schematic illustration for the exfoliation of graphite through ball milling approach. Source: Based on León et al. [62].

required to break the enormous van der Waals-like forces between the graphite layers [59]. Current techniques produce graphene in both *bottom-up* and *top-down* approaches [60]. *Bottom-up* methods include chemical vapor deposition (CVD) or epitaxial growth on a substrate and tend to produce high-quality graphene films.

In contrast, *top-down* approaches have been explored to exfoliate graphene nanosheets from graphitic precursors. Within this class, the use of an aromatic amine, along with the mechanical activation achieved by milling process, has been recently applied to the exfoliation of graphite [61]. Specifically, it was shown that large quantities of inexpensive materials, namely, graphite and melamine (2,4,6-triamino-1,3,5-triazine), can be used for the massive and fast production of concentrated dispersions of FLG with a low amount of defects (Figure 8.7) [62]. In a typical procedure, a solid mixture of melamine and graphite is ball-milled under air atmosphere. Thus, the adsorption of melamine on graphene is the key step to compensate the huge van der Waals attractive interactions between the layers, thereby allowing the exfoliation process [63]. Then, the resulting solid mixture was dispersed in DMF (or water) producing a black concentrated suspension, which contained the desired FLG.

8.3.5 Other Carbon Nanomaterials

In the family of carbon allotropes, other "minor" members have their own identity and their potential applications. Among them, carbon nanohorns (CNHs), nanodiamonds and CNOs must be mentioned. In general, their reactivity is quite similar to that of the most famous siblings fullerenes, CNTs, and graphene. For this reason, they have been functionalized either covalently or noncovalently using many of the synthetic strategies developed for CNTs and graphene, as we illustrate in the following paragraphs.

8.3.5.1 Carbon Nanohorns

CNHs are conical-shaped carbon nanostructures sometimes also called carbon nanocones constituted by one or more sp^2 carbon sheets typically 2–5 nm in diameter and 40–50 nm in length (see Figure 8.8 for an example of transmission electron micrographs). CNHs belong

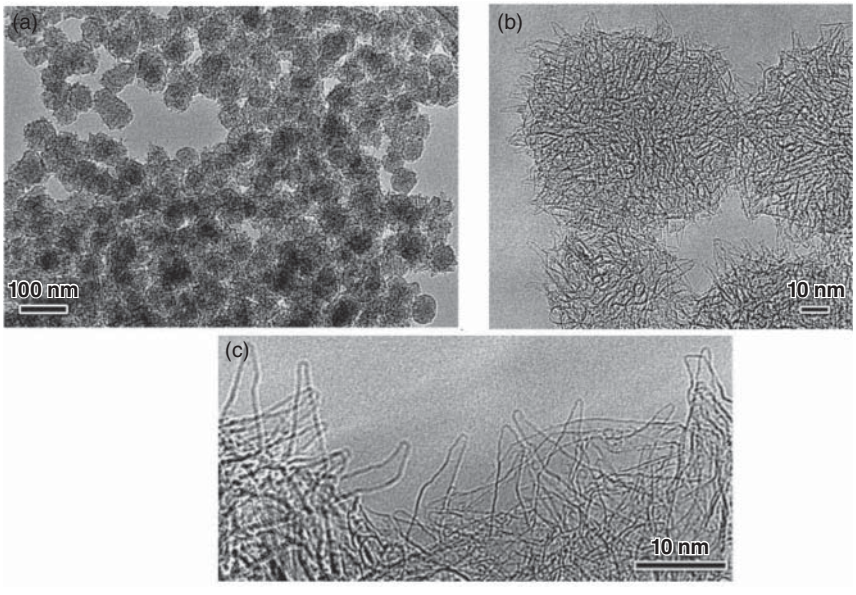

Figure 8.8 Transmission electron micrographs of carbon nanohorns: (a) close-up of individual nanohorns, (b) aggregates of nanohorn clusters, and (c) zoom-in on a few aggregates of nanohorns, also known as dahlias, produced by laser ablation. Source: Reprinted from Iijima et al. 1999 [64]. Copyright 1999, Elsevier.

to the group of one-dimensional carbon nanostructures, but during the synthesis, they can aggregate into spherical clusters ~100 nm in diameter called "dahlia-like" clusters. CNHs have been first observed by Harris et al. from the waste product of soot formed during the production of fullerenes via arc discharge process [65]. After heating to 2500–3500 K with positive-hearth electron gun for approximately four hours, the soot is converted into two types of nanohorns, single-walled carbon nanohorns (SWCNHs) and multiwalled carbon nanohorns (MWCNHs).

"Dahlias" of nanohorns were first synthesized via laser ablation process of graphite in an argon atmosphere by Kasuya and coworkers. CNHs are apt to industrial take-up. Notably, they can be produced cheaply, in large quantities, without the need for subsequent purification steps and without the presence of metal catalysts [66]. CNHs are considered as a good replacement of CNTs because of their large specific surface area, high production yield, high chemical stability, high purity, low toxicities, exceptional catalytic properties, superior porosity, and good conductivity. Because of all these properties, CNHs found applications in the fields of electrochemical sensing or biosensing, biofuel cell development, as an electrode material, supercapacitor, gas storage devices, and biomedical application [67]. CNHs have been modified with amino groups similarly to the previously described carbon-based nanomaterials: oxidized CNHs were conjugated to the fifth generation of polyamidoamine (PAMAM) dendrimer and used as an essential substrate for the incorporation of Pd^{2+} ions, which were subsequently chemically reduced to Pd nanoparticles.

The latter dendrimer-encapsulated Pd nanoparticles onto oxidized CNHs were efficiently employed as nonenzymatic tracing tag for the electrocatalytic reduction of dissolved oxygen

[68]. Oxidized CNHs, after activation with *N*-ethyl-*N*′-(3-(dimethylamino)propyl) carbodiimide hydrochloride (EDC) and 1-hydroxy benzotriazole (HOBt), were treated with *tert*-butyl 2-(2-(2-aminoethoxy)ethoxy)ethylcarbamate for the preparation of modified CNHs carrying amines masked by BOC protecting groups [69]. Acidic deprotection of the BOC moieties liberated free amines on the modified CNHs, which were subsequently conjugated with 5,10,15-tris(3,5-di-tert-butylphenyl)-20-[4-(carbonyloxy)phenyl] porphyrin, providing a donor–acceptor CNH-based hybrid, with significant redox and photophysical properties. Oxidized CNHs carrying ammonium groups were assembled to a benzo-18-crown-6-ether moiety linked to a pyrrolidine-functionalized C_{60} [70]. The so-formed C_{60}-CNH nanohybrid similarly showed high dispersibility in organic solvents, which allowed its spectroscopic characterization. In addition, femtosecond laser flash photolysis disclosed efficient electron transfer events from the singlet excited state of the C_{60} unit to CNHs, thus indicating the action of the CNH moiety as an electron donor and C_{60} as an electron acceptor, effectively facilitating charge-separation while suppressing the recombination of photoexcited electron–hole pairs.

Many studies are dedicated to the covalent functionalization of CNHs sidewalls with amino groups. Large aggregates of CNHs were successfully deagglomerated and solubilized in aqueous media after treatment with $NaNH_2$ in refluxing liquid NH_3, which resulted in the introduction of amino groups onto their outer surface [71]. The so-formed amino-modified CNHs were further derivatized with the fluorescent dye Oregon Green and incubated with growing mammalian cells (3T3 and HeLa cells), revealing low cytotoxicity. Furthermore, the covalent attachment of a biotinylated diamide onto amino-CNHs through an amidation reaction led to a biotinylated CNH intermediate, which proved to be an excellent specimen for the conformational study of such modified CNHs by TEM imaging (Figure 8.9) [72].

Acidic deprotection of BOC-protected amino-modified CNHs allowed their labeling with fluorescein isothiocyanate (FITC), which made them useful for monitoring their interaction with primary murine macrophages. In a similar approach, 2,2′-(ethylenedioxy)bis(ethylamine) was directly cross-linked with intact CNHs using a simple bath sonication method for 10 hours [73]. Subsequently, such amino-functionalized CNHs were conjugated with the fluorescent IR Dye 800 CW via an amidation reaction, thus constructing a light-driven nanomodulator that generates heat and reactive oxygen species under biologically transparent near-infrared laser irradiation.

1,3-Dipolar cycloaddition of azomethine ylides, in situ generated upon thermal condensation of aldehydes and α-amino acids, was also employed for the modification of the sidewalls of CNHs with amino groups. With this particular cycloaddition reaction, a large number of pyrrolidine units fused to C—C bonds on the CNH sidewalls were introduced, affording highly dispersible functionalized materials. Most importantly, a significant variety of pyrrolidino-modified CNHs with diverse substituents on the pyrrolidine ring can be prepared, depending on the nature of the utilized aldehyde and/or α-amino acid. Thus, different aldehydes give rise to functionalized CNHs carrying diverse substituents on the α-carbon atom of the pyrrolidine ring, while N-modified α-amino acids lead to different N-substituted pyrrolidines on the skeleton of CNHs [74]. One example of this kind of derivatives was reported as a new selective antibody–drug nanosystem based on CNHs for the treatment of prostate cancer (PC) [75]. In particular, cisplatin in a prodrug form

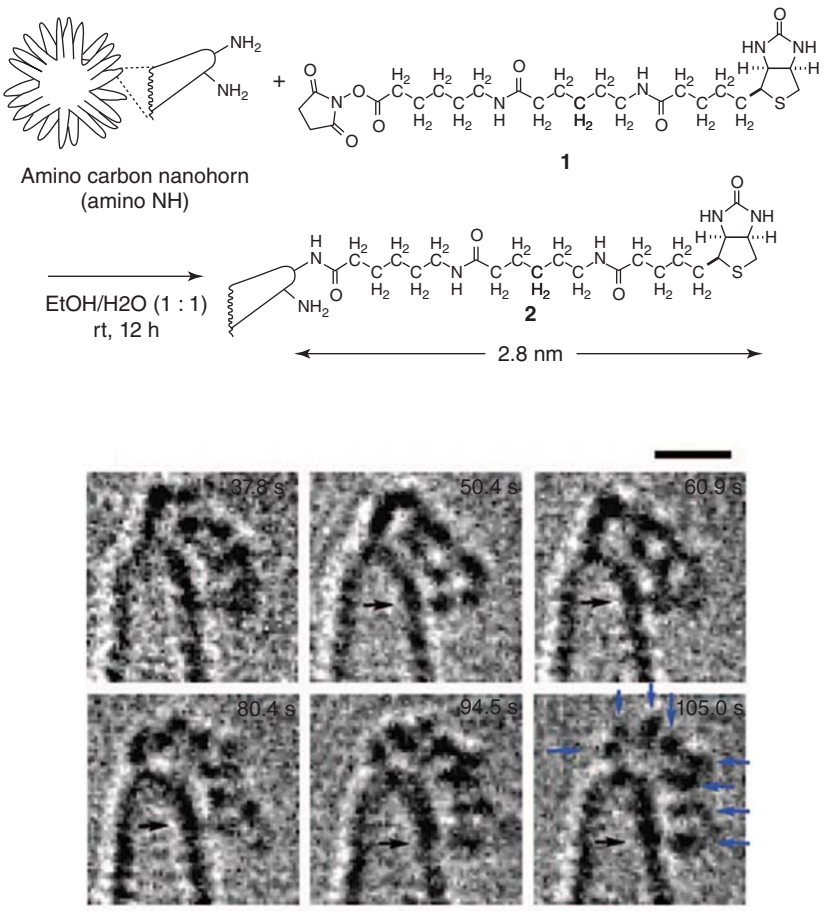

Figure 8.9 TEM images of triamide–NH conjugate in a series of bent conformations. The figure captions refer to the time (seconds) after initiation of the observation, i.e. initiation of electron irradiation. Source: Reprinted with permission from Nakamura et al. [72a] and Lacotte et al. [72b].

and the monoclonal antibody (Ab) D2B, selective for prostate-specific membrane antigen (PSMA) + cancer cells, have been attached to CNHs because of the current application of this antigen in PC therapy. The hybrids Ab–CNHs, cisplatin–CNHs, and functionalized CNHs have also been synthesized to be used as control systems. The efficacy and specificity of the D2B–cisplatin–CNH conjugate to selectively target and kill $PSMA^+$ prostate cancer cells compare very well with other derivatives.

The radical addition of in situ generated aryl diazonium salts was applied to covalently modify the outer skeleton of CNHs. By this method, the thermally induced reaction of pristine CNHs with aryl diazonium intermediates, generated in situ from aniline derivatives after treatment with isoamyl nitrite, resulted in the covalent grafting of a wide range of aryl units onto the outer walls of CNHs, thus enhancing their solubility in common solvents. Following this procedure, either simple anilines, such as 4-nitroaniline, 4-aminobenzoic acid, and 4-butylaniline, or more complex aniline derivatives, such as

tert-butyl (2-(2-(2-(4-aminobenzamido)ethoxy)ethoxy)ethyl)carbamate, were reacted with CNHs in the presence of isoamyl nitrite in a mixture of *o*-dichlorobenzene/acetonitrile as solvent to afford novel highly functionalized hybrid materials [76].

Recently, microwave-assisted chemistry proved to be a powerful tool toward chemical functionalization of carbon nanostructured materials, presenting significant advantages by shortening considerably the reaction times and offering higher yields and/or fewer by-products. Furthermore, taking advantage of the strong microwave absorption that carbon nanostructures exhibit, the presence of toxic and irritant solvents can be reduced, thus establishing microwave-assisted chemical functionalization as a general concept in green chemistry. Therefore, without surprise, most of the already known reactions that conventionally take place for the chemical modification of CNHs were also tested with the aid of microwave irradiation. In this line, the 1,3-dipolar cycloaddition of in situ generated azomethine ylides onto the outer surface of CNHs was achieved by using microwave irradiation in the absence of any solvent and within one hour of reaction time. The latter result was a significant improvement compared with the corresponding conventional methodology, which takes place in DMF as a solvent and needs thermal treatment for more than 100 hours [77]. In the same report, the introduction of various aryl units onto the CNH-surface via the radical addition of in situ generated aryl diazonium salts was achieved with the aid of microwave irradiation and in environmentally friendly aqueous media. In a further step, taking advantage of the fact that the cycloaddition reaction was more selective and slower than the radical addition, the double functionalization of CNHs, namely, the 1,3-cycloaddition under solvent-free conditions, followed by the radical addition of aryl diazonium salts in water, led to multifunctionalized hybrid materials with great potential in diverse applications.

8.3.5.2 Carbon Nanodiamonds

Carbon nanodiamonds (CNDs) are in the group of zero-dimensional carbon nanoallotropes, consisting primarily of tetrahedral sp^3 carbon atoms. They have a diamond-like monocrystalline topology with crystal domains and particle size less than 10 nm. Nanodiamonds consist of complex structures with an inner diamond core and an outer amorphous carbon shell. Because of this type of structure, they display unique properties such as high surface area, hardness, high electrochemical stability, mechanical robustness, high thermal conductivity, environmental inertness, high insulating capability, modifiable color centers, nanotribology, thermal expansion, chemical corrosiveness protection, nontoxicity, and biocompatibility [78].

Nanocrystalline diamonds are characterized by an irregular shape and, depending on the synthesis and purifications, different populations of nanometer-sized materials can be recovered. The shape of ultrananocrystalline particles is almost spherical, with an average size equal to 5 nm. By high resolution transmission electron microscopy (HRTEM), the diamond core is easily recognized. HRTEM can be also helpful to pinpoint structural defects inside the nanoparticles (Figure 8.10) [80].

Nanodiamonds can be produced by the detonation method, laser ablation, CVD, high impact on diamond microcrystals, ball milling, meteoritic impacts process, jet milling, or abrasion of microdiamonds. Nanodiamonds offer a potential novel template for drug delivery and targeting because of their small primary particle size, purity, excellent

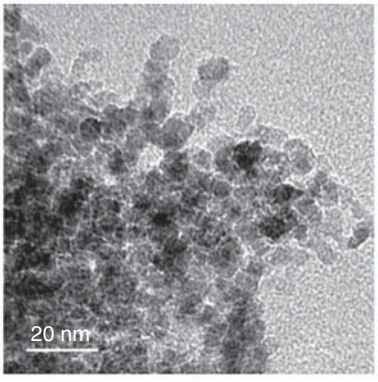

Figure 8.10 TEM micrograph of 10 nm diameter nanodiamond. Source: Reprinted from Valey et al. [79].

properties, facile surface functionalization, high biocompatibility, and inexpensive large-scale synthesis.

However, nanodiamond properties such as aggregation state, surface chemistry, and presence of impurities, as well as the localization and accumulation behavior at the organism level, must be controlled to maintain safety and retain efficacy of conjugated therapeutic agents.

Nanodiamonds functionalized with different organic moieties carrying terminal amino groups have been synthesized. Fluorinated nanodiamonds can further react with ethylenediamine, resulting in amino-nanodiamond [81]. Alternatively, carboxylated NDs were linked to ethylenediamine via acyl chloride intermediate [82]. Reaction of aminated NDs with epoxy resin results in covalent incorporation of the ND into a polymer network. Covalently bonded nanodiamond-epoxy composites showed a three times higher hardness, 50% higher Young's modulus, and two times lower creep compared to the composites in which the nanodiamond was not chemically linked to the matrix.

For the quantification of primary amino groups, a modified photometric assay based on the Kaiser test has been developed and validated for different types of aminated nanodiamonds. The results match well with the values obtained by thermogravimetry analysis. The method represents an alternative wet-chemical quantification method in cases where other techniques, such as elemental analysis, fail because of unfavorable combustion behavior of the analyte or other impediments [8d].

Another method to obtain more homogeneous nanodiamond surfaces is the reduction of surface carbonyl groups. Kruger et al. reported on the reaction with borane, leading to hydroxylated diamond samples [83]. This material can be modified in a variety of ways. The grafting of trialkoxysilanes easily yields functionalized nanodiamond particles. The reaction can be carried out with different silanes, for example, trimethoxy- and triethoxy-3-amino-propylsilane. The amino groups of the material are accessible for further surface modification. Besides the build-up of a short model peptide on the diamond solid phase, biotin was covalently immobilized on the particle surface by coupling with the amino groups of the silane. Its activity in the binding to streptavidin was demonstrated, making it a model for bioactive moieties covalently grafted onto the diamond surface. An interesting application of amino-functionalized ND was reported by Yu et al. To align the effective nanocarrier features of the supraparticles (SPs) with alkyl amine molecules,

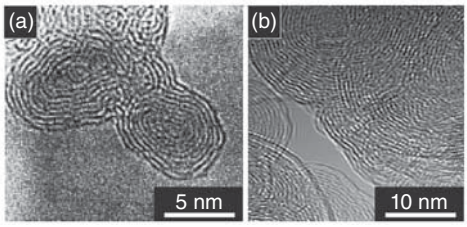

Figure 8.11 TEM images of carbon nano-onions. Source: Reprinted with permission from Plonska-Brzezinska [86].

carboxylic ND (ND-ori)-based supraparticles (ND-SPs) were designed and synthesized via a condensation reaction between the carboxylic group on the surface of ND-ori and the amino group of the primary alkyl amines, *n*-octylamine (Oct), dodecylamine (Dod), and oleylamine (Ole) [84]. Alkyl amine molecules have indeed a relatively lower bioaccumulation compared to fluorine compounds usually employed to achieve this kind of entities [84a]. Oct-ND-SPs and Dod-ND-SPs spontaneously self-assembled in SP and were used for further drug efficacy tests because of their low cytotoxicity. A model anticancer drug camptothecin (CPT) was incorporated into these ND-SPs and conventional polyethylene glycol (PEG)-modified polymer micelles, and the ND-SPs showed good drug efficacy against U_2OS bone osteosarcoma cells. In particular, CPT-loaded ND-SPs displayed the highest anticancer therapeutic effect. In vivo antitumor assays showed that CPT delivered by ND-SPs caused stronger tumor suppression of HT-29 colorectal adenocarcinoma xenografts.

8.3.5.3 Carbon Nano-onions

CNOs are essentially multilayer fullerenes, which were first observed by the Ugarte group in 1992 [85]. CNOs consist of spherical closed carbon shells, multilayered, quasi-spherical, and polyhedral shaped shells with structure resembling that of an onion (Figure 8.11). CNOs are totally insoluble in organic and inorganic solvents, similar to SWNTs. This lack of solubility hinders the study of their chemical and physical properties.

Currently, the most common method used for the production of spherical CNOs is the method based on annealing ND particles (average diameter of 5 nm) at high temperatures in an inert atmosphere under a high vacuum, frequently called the Kuznetsov method (named after the creator of this method) [84b].

The first covalent functionalization of CNOs was reported in 2003 by Georgakilas et al. using the 1,3-dipolar cycloaddition of azomethine ylides [87]. A few years later, an azomethine ylide addition reaction was used for nanodiamond-derived CNOs [88]. *N*-Boc-protected amino-CNO-pyrrolidine was synthesized using the procedure proposed by Prato and coworkers for the synthesis of fullerene derivatives (Figure 8.12a) [21b]. Functionalization at defect sites is also possible exploiting the carboxylic acid moieties present therein to link polymeric and oligomeric functional groups. For further successful reactions with amino-terminated compounds, the presence of these carboxyl groups is very crucial because a considerable difference between nanotubes and CNOs is, of course, the fact that the latters do not have easily accessible open ends, which facilitate oxidation. Under conditions similar to those reported for the direct functionalization and solubilization of single-walled CNTs by diamine-terminated PEG [89], CNOs could be

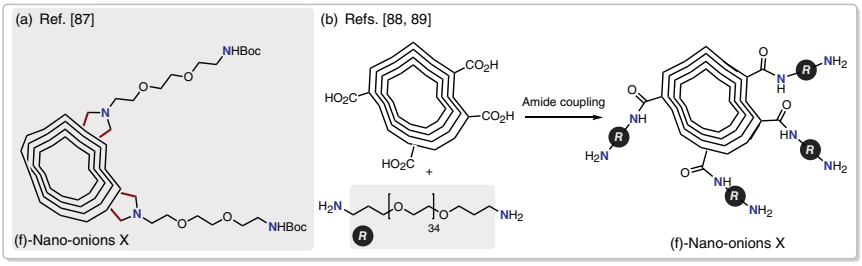

Figure 8.12 Amino functionalization of CNO by (a) cycloaddition reaction on nano-onions. Source: Based on Georgakilas et al. [87]. (b) Amide coupling on nano-onions. Source: Cioffi et al. [88] and Huang et al. [89].

made water soluble [90]. The CNOs were allowed to react at 140 °C for reaction times up to 19 days (Figure 8.12b).

8.3.6 Amino-Functionalized Carbon-Based Nanomaterials for Analytical Applications

The sensitivity of the electronic properties of CNT toward molecules adsorbed on their surface, and the high surface area providing for this high sensitivity, make CNT a promising starting material for the development of superminiaturized chemical and biological sensors [91]. The operation principle of these sensors is based on changes in the V–I curves of nanotubes as a result of adsorption of specific molecules on their surface. The use of CNT in sensor devices is one of the most promising applications in electronics and the functionalization with amino groups has often provided a good improvement in the performances.

The nitrogen dioxide (NO_2) gas sensitivity of monolayer CNT functionalized by the amino group $–NH_2$ was studied [92]. The amino group acts as a charge transfer agent of the semiconducting CNT that increases the number of electrons transferred from the nanotube to the NO_2 molecule.

A CNT-PAMAM hybrid obtained by covalently linking PAMAM onto CNTs has demonstrated to be useful for preparing multiple nanocomposites and for carrying biomacromolecules for different purposes. Zeng et al showed that they can be very effective as platform components of biosensors. The GO_x and horseradish peroxidase (HRP) immobilized CNTs-PAMAM show excellent performance for glucose sensing detection. The dispersion of the hybrid possesses excellent stability in water because of the large number of amino groups on the surface of the CNT-PAMAM. The amino groups on the CNT-PAMAM can be easily regulated by using different generations of PAMAM [93].

Graphene and its derivatives have generated a great deal of interest in the field of analytical sensors, mainly thanks to their unique physicochemical features [12, 94]. Indeed, both the large surface area and planar geometry of these carbon-based materials may generally enhance the loading of targeted molecules (gas and liquid), thus resulting in improved detection abilities [95]. As an example, the superficial functionalization of graphene with numerous amino groups has been recently used to produce a gas sensor for the detection of formaldehyde, which is the most common indoor pollutant gas and harmful to human health [96]. The superficial amines on this graphene-based sensor may therefore react with

the gaseous formaldehyde to provide the corresponding imine adducts, thus allowing the detection of the target analyte.

8.4 Amines in the Synthesis and Functionalization of Carbon Dots

In recent years, carbon dots (CDs) have emerged as a new class of carbon-based nanomaterials [97]. CDs are quasi-spherical nanoparticles with dimensions below 10 nm. They are typically composed mostly of carbon and oxygen atoms, but doping with other types of atoms – in particular nitrogen – is commonly encountered, affording improved properties.

CDs have been isolated serendipitously from the purification of SWCNTs obtained from arc discharge [98]. Their synthesis is indeed possible with the so-called top-down methods, such as laser ablation, arc discharge, and electrochemical oxidation of larger carbon structures. On the other hand, it has become clear that similar materials can also be obtained from the thermal treatment of small molecular precursors [99]. These synthetic routes include pyrolysis and hydro- or solvothermal synthesis. In contrast with top-down methods, the bottom-up strategies offer more precise control over the final material. In our experience, microwave hydrothermal treatments provided quick and highly reproducible syntheses, with the possibility to include additional molecular doping agents directly during the synthesis. This allowed to obtain materials tailored for specific applications [100]. Indeed, some properties such as luminescence, and the functional group present on CDs, can be controlled at least to some extent with a proper choice of the molecular precursors. Common precursors are citric acid, amino acids, urea, simple aliphatic amines, and small aromatic molecules, such as aniline and phenol derivatives.

For what concerns the synthetic conditions, the use of high temperature is a consistent trend, with the employed temperatures in most cases being above 140 °C. High temperature promotes the formation of a carbonaceous core, following cross-linking and aromatization. Under hydrothermal conditions, 300 °C may be considered as a boundary temperature: lower temperatures are associated with the formation of amorphous, sp^3 carbon-rich CDs, while higher temperatures promote the formation of more graphitic materials. The time also affects the properties of the final material. In this case, longer reaction times lead to more graphitic CDs, while shorter times are associated with amorphous materials. Common synthesis times range from a few hours up to a few days. In this regard, microwave-assisted reactions have demonstrated their potential, allowing to shorten considerably the required time, down to a few minutes, providing a quick access route to this class of nanomaterials.

At present, the formation mechanism of CDs remains largely unknown and is currently under investigation [101]. As a consequence, the control on the synthesis is also limited, albeit some general trends have emerged. One consistent element is the presence of polar superficial groups, such as acids, alcohols, and amines, which provide solubility in water and polar solvents. This is typically inferred from IR data, combined with XPS analysis. The second element that emerges rather consistently from the literature is that some of the moieties present in the molecular precursors are retained during the synthesis [97]. This is a first element that allows tuning the properties of the final material depending on the starting mixture of precursors.

The possibility to tune the properties of the final materials directly during the synthetic process is one of the reasons why CDs have stimulated a growing interest among scientists. Indeed, in most nanomaterials, the functionalization has to be performed at later stages, as discussed also in the initial part of this chapter. For this aim, as well as for the engineering of specific functional properties, the amino group has proven extremely versatile.

8.4.1 Amines as CD Constituents

Soon in the development of CDs, the use of a molecular precursor bearing acidic functionalities, such as citric acid, has been combined with the use of amino groups. Under the commonly employed hydrothermal conditions, the formation of amide bonds can occur, leading to oligomeric structures. Despite the detailed mechanism of formation of CDs is unknown and is currently the subject of debate, it seems reasonable to envision a polymerization, followed by aromatization reactions that lead to graphitic structures. Experimentally, the degree of graphitization is inferred from XPS data, TGA, and TEM images [102]. The latter technique has allowed imaging nanoparticles with layered graphitic structures.

The concept of polymerization followed by aromatization is also consistent with extensive screening of synthetic conditions that indicated multifunctional small molecule units as precursors of election, bearing complementary units, such as acid and amine, or amine precursors, such as urea, that is known to undergo thermal decomposition to give ammonia and isocyanic acid under hydrothermal conditions. Indeed, two of the most studied combinations of CDs precursors are citric acid with either ethylenediamine or urea [103]. In these cases, the nitrogen-containing precursor is considered a nitrogen doping agent because it introduces the heteroatom in the CD structure. The combination of ethylenediamine with citric acid is a particularly significant case. Indeed, these two precursors have been frequently used jointly, and their reaction has been studied in considerable more detail than other systems. In this case, amide formation occurs readily, followed by a cyclization reaction, ultimately leading to the formation of 5-oxo-1,2,3,5-tetrahydroimidazo[1,2-α]pyridine-7-carboxylic acid (IPCA) [103]. This small molecule is highly fluorescent and has been identified by several authors as a product formed under the employed synthetic condition of CDs from citric acid and ethylenediamine [104]. In particular, IPCA was observed after purification of the reaction products by column chromatography, and analysis of the prominent fluorescent fraction by NMR and mass spectrometry [105]. IPCA has therefore been identified unambiguously as the principal fluorescent unit of that type of carbon dots. Whether this small fluorophore is present as a single entity, it is entrapped or is covalently bound to a carbon-based polymeric matrix remains unclear. Fluorescence correlation spectroscopy studies suggest that the fluorophore is present as an independent unit [106]. Similar conclusions have been reported for CDs obtained from citric acid and urea. Indeed, it has been observed that a thorough purification protocol is required in the preparation of these nanomaterials because of the "ubiquitous" presence of fluorescent impurities that originate during the synthesis [107].

The use of amino acids as precursors seems to partially overcome this issue. Several amino acids have been used to prepare CDs. These include histidine, aspartic acid, arginine, lysine, and cysteine, among others [108]. In the case of amino acid, an obvious role of CDs is to serve as polymerization units via amide bond formation. However, additional roles have

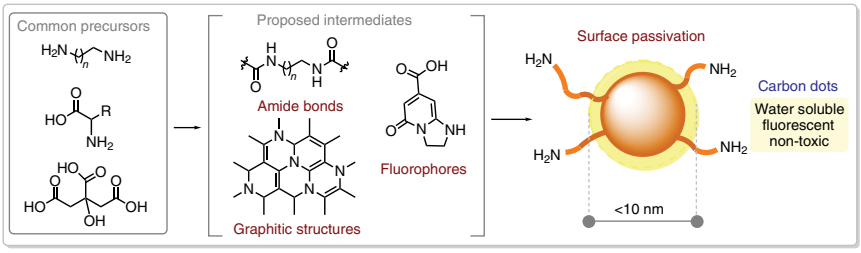

Figure 8.13 Role of amine precursors in the synthesis of CD. Depending on the synthetic conditions and the chosen precursors, intermediate structures can form, such as oligomers, molecular fluorophores, and graphitized N-doped structures. When the synthesis is performed at relatively low temperature (i.e. below 300 °C), the amines may have the role of passivating agents.

also been attributed to amine precursors, in particular in relation to the luminescence of CDs (Figure 8.13).

A consistent observation is that heteroatom doping, and in particular nitrogen doping, affords better luminescence properties, i.e. higher quantum yields. In amorphous CDs, this effect is related to the formation of fluorophores, whereas in graphitic systems, it has been associated with the emission of N-centered defects in the structure [109]. Even beyond the simple analysis of quantum yields, a clear example of the useful transformation of amino groups into graphitic structures has been reported by Reisner and coworkers, who studied graphitic carbon dots obtained from a prolonged thermal treatment above 300 °C, using either citric acid or aspartic acid as single-source precursors [108]. In both cases, CDs with a comparable size of c. 3 nm were obtained, with those obtained from aspartic acid displaying clear lattice fringes. XPS data revealed that nitrogen was included in the structure only as pyridinic or pyrrolic units. These N-doped CDs were used as photosensitizers for photocatalytic hydrogen evolution and displayed enhanced absorption in the visible region of the electromagnetic spectrum, as well as better photosensitizer abilities.

A complementary role is attributed to nitrogen (mostly amine)-doping in the synthesis carried out at lower temperatures. In these cases, amines are described as passivating agents that protect the photoactive core of CDs from the surrounding environment. Indeed, several studies have demonstrated the importance of passivation to enhance the CD properties, and amines emerged as one of the best performing passivating agents [110]. In a comparative study, citric-acid-based CDs were synthesized at temperatures close to 200 °C, adding ammonium hydroxide, ethylenediamine, or diethylenetriamine as doping agents [111]. The authors observed that the use of primary amine could boost the luminescence quantum yield, which increased from below 1% in the case of nonpassivated CDs, up to above 50% when the triamine was used. Interestingly, increasing the amount of triamine increased the quantum yield almost linearly. On the other hand, amine passivation decreased the photostability of the material. In the same study, electrophoretic experiments revealed negatively charged CDs and CDs with both positive and negative charge, indicating that what is described as surface passivation, or doping, most likely reflects a broad range of chemical reactions, leading to a multitude of different structures. Indeed, for simple surface passivation, one would expect a net positive charge, uniformly present on CDs. To this aim, CDs obtained solely from the thermal treatment of polyamines, which could be successfully used

in biological application such as gene delivery, owing to the charge complementarity with nucleic acids, have been prepared [112].

8.4.2 Amine-Rich CDs from Arginine and Ethylenediamine (NCDs)

Considering the role of amino groups in amide bond formation, graphitization, and passivation, our group focused on the engineering of nitrogen-doped CDs obtained from the microwave-assisted hydrothermal synthesis of arginine and ethylenediamine (nitrogen-doped carbon dots, NCDs) [100, 113]. A short treatment (three minutes) at 240 °C of the precursors, mixed with a minimal amount of water, turns the light yellow mixture into a brown solution, which is purified by filtration and dialysis. The resulting NCDs were imaged with atomic force microscopy (AFM), revealing small particles with a size of 2.5 ± 0.8 nm, having good solubility in water, and sufficient solubility in polar organic solvents such as methanol and DMF. These NCDs displayed a good quantum yield of 0.17, which could be increased up to 0.46 upon chromatographic separation of different families of NCDs. Additional structural information was obtained by NMR experiments performed with ^{13}C-labeled precursors. These experiments revealed that the aromatic domains of NCDs mostly originated from arginine, whereas the carbon atoms of ethylenediamine were associated with aliphatic portions of the material. XPS analysis revealed the presence of nitrogen in different forms. Importantly, this material provided a positive Kaiser test, leading to the quantification of 1350 μmol/g of primary aliphatic amines. The oxidation potential of NCDs is consistent with the presence of primary amines. A combination of NMR and electrochemical studies indicated that these amines are somehow similar to benzylamine or phenethylamine [114]. Despite the importance of this rationalization, it is stressed that it should be taken with great caution, considering the complexity of the system under study, and the extremely limited knowledge of its structural features. Having established the presence of amines even in the final material, it became possible to exploit the amino group for different purposes, during the synthesis, or in postfunctionalization [100].

8.4.2.1 One-Pot Functionalization of NCDs

A particularly attractive strategy to tailor the properties of NCDs is to exploit the reactivity of the amino group to incorporate the desired molecular units directly during the synthesis (Figure 8.14).

A significant example of the exploitation of amino groups of NCDs during the synthesis has been their reaction with naphthalene dianhydride (either bare or substituted) [115]. Reaction of ethylenediamine to form naphthalene diimides was expected under the synthetic conditions employed, and the resulting imides could further participate in NCD formation, leading to the inclusion of the naphthalene-based chromophore in the final nanomaterial. The envisioned reactivity was indeed observed, leading to NCDs emissive in the blue or orange region of the spectrum, depending on the substitution pattern of the starting anhydride. Computational insights suggested that when a naphthalene dianhydride precursor bearing bromide substituents in the bay region was employed, amine could participate in nucleophilic aromatic substitution reactions. By adjusting the ratio between two different anhydride precursors, white-light-emitting NCDs were obtained. Overall, this proved to be

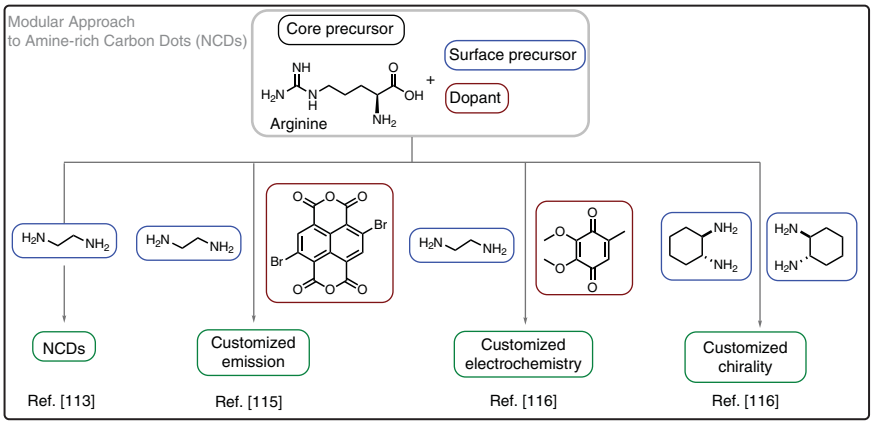

Figure 8.14 Examples of doping strategies to tailor the properties of NCDs during the synthesis, exploiting the amino group reactivity, with acids, anhydrides, electron-poor aromatic groups, and quinones.

an effective strategy to exploit the reactivity of the amino precursors tailoring the absorption and emission properties of the nanomaterial.

Using a conceptually analogous strategy, the redox properties of NCDs could also be modulated [116]. In this case, quinones were used as doping agents, which could react with amines to afford the corresponding imine derivatives. Introduction of quinones in the reaction mixture afforded NCDs with less negative reduction potentials, which could be modulated from −1.52 to −2.04 V vs. saturated calomel electrode (SCE). The oxidation potentials were also affected by the doping procedure. This is coherent with the participation of the amino groups in the formation of adducts with quinones during the synthesis, thus limiting their availability to undergo oxidation as such.

As a final example of modification during the synthesis, chirality was controlled using a chiral diamine, i.e. (*R*,*R*)- or (*S*,*S*)-cyclohexanediamine, instead of ethylenediamine [117]. Albeit conceptually simple, the inclusion of chiral precursors into CDs is not straightforward because of the harsh synthetic conditions that are typically required for the synthesis of CDs. Indeed, even if in our standard protocol (*S*)-arginine is employed, racemization occurs during the synthesis, despite its short time (three minutes). In fact, most of the chiral CDs reported rely on postsynthetic modifications. On the contrary, (*R*,*R*)- and (*S*,*S*)-cyclohexanediamine retained their chirality at least to an extent that was appreciable spectroscopically, by both electronical circular dichroism (ECD) and vibrational circular dichroism (VCD). In addition, the obtained chiral nanomaterials could be effectively employed to transfer their chirality to a supramolecular polymer.

Overall, from these examples, it should emerge the versatility of the amino group in the synthesis of NCDs as a mean to tailor the functionality of the final material via small-molecule doping.

8.4.2.2 Postfunctionalization of NCDs

Besides in-synthesis doping, postfunctionalization strategies are also extremely useful to embed specific functionalities to the nanomaterial (Figure 8.15) [108, 118]. This route is

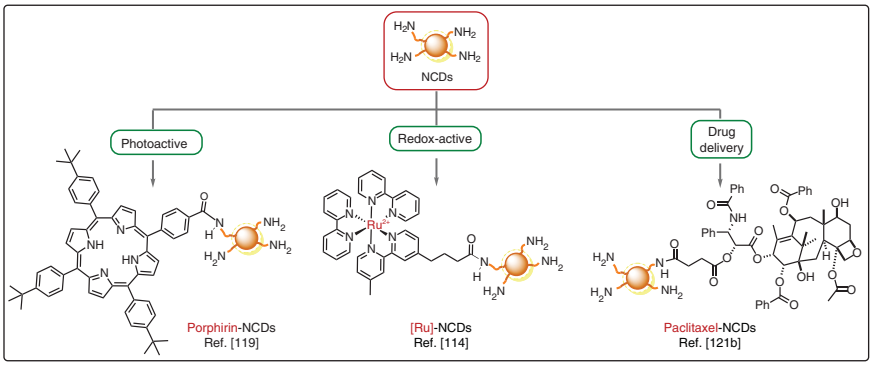

Figure 8.15 Examples of nanoconjugates obtained from the coupling of functional units to NCDs via amide bond formation.

particularly attractive to introduce residues that may degrade during the synthesis or interfere with it, as well as units that benefit from the interaction with the CD platform. Moreover, this strategy offers a much better control on the molecular structures present in the final material because the fragment introduced at the postfunctionalization stage retains its defined molecular structure. One of the first development envisioned, in these regards, has been the use of NCDs in a covalently bound photoactive nanoconjugate for charge separation purposes [119]. Porphyrin was selected as a coupling partner because of its proven ability to be engaged in electron transfer processes [120].

Covalent functionalization was achieved in a straightforward manner by coupling a porphyrin derivative bearing a pendant carboxylic acid via amide bond formation promoted under classical coupling conditions.

In the resulting nanoconjugate, detailed spectroscopic analysis revealed that upon light excitation, a charge-separated state formed. In this state, the positive charge is localized on the porphyrin, while the negative charge is localized on the NCD. This observation may seem counterintuitive for an amine-rich nanoparticle because the pendant groups are prone to oxidation. This partially unexpected behavior further highlights the complexity of NCDs as nanomaterials.

The capability of NCDs to undergo oxidation was exploited in a different nanohybrid, in which a derivative of ruthenium(II)tris(2,2′-bipyridyl) ($Ru(bpy)_3^{2+}$) bearing a pendant carboxylic functionality was covalently attached to NCDs [114]. In this case, the nanohybrid was exploited in the efficient generation of electrochemiluminescence (ECL). Indeed, the metal complex is a well-known luminophore in this context, which usually operates in the presence of an oxidizable coreactant. Alkyl amines are the most representative class of coreactants but have some drawbacks, e.g. the commonly employed tripropylamine is toxic, corrosive, and volatile, while it has to be used in high concentration. On the contrary, use of the nanohybrid as an ECL platform allowed the system to operate via an intramolecular electron transfer, leading to an enhanced ECL signal compared to the separated components, without the need to employ toxic amines in high concentration.

Besides the engineering of photophysical and electrochemical processes, the postfunctionalization of superficial amines can also be employed for the conjugation of drugs,

leading to the formation of a prodrug [121]. The use of NCDs as a drug delivery system is particularly attractive, given their water solubility, low toxicity, and fluorescence, which in principle may allow to monitor the localization of the conjugate. In particular, studies in our group focused on the delivery of paclitaxel because it is a drug with poor water solubility, which could thus benefit from the conjugation to a highly water-soluble platform [121b]. Upon derivatization of paclitaxel with succinic anhydride at the hydroxyl C2′ position, the residual pendant acidic moiety was again used to conjugate the nanohybrid via amide bond formation. Successful conjugation was confirmed via a number of techniques, including diffusion-ordered NMR spectroscopy, matrix-assisted laser desorption ionization, and AFM. The hybrid nanomaterial-induced apoptosis in cancer cells, displaying a slightly better anticancer activity compared to the drug alone, evaluated in breast (MCF-7 and MDA-MB-231), lung (A-549), prostate (PC-3), and cervix (HeLa and C33-A) cancer cell lines. Because the drug is known to be inactive when the 2′ hydroxyl moiety is derivatized, the hybrid is likely active only upon ester hydrolysis.

8.4.2.3 Use of CD-Supported Amines in Organocatalysis

Amino groups are prominent in organocatalysis [122], as also reported elsewhere in this book. Their support on CDs as aminocatalytic platforms would be an advantage, in particular aiming at their uses as organocatalysts in biological media. One tantalizing opportunity enabled by this process is in situ drug synthesis [123]. The exploitation of amino groups in the context of CD-promoted organocatalysis is still in its infancy, albeit some applications related to catalysis started to emerge [124]. In our group, amine-rich NCDs have been employed for the photocatalytic perfluoroalkylation of electron-rich substrates, including phenols, olefins, and caffeine [125]. In this case, the important role played by the superficial amino groups is related with its ability to engage in halogen bond interactions with iodoperfluoroalkyl substrates, as supported by ^{19}F-NMR experiments. The proximity of the substrate facilitates electron transfer from the excited state of NCDs to the iodinated substrate, generating a highly reactive perfluoroalkyl radical. Overall, this strategy allowed the formation of C—C bonds under mild and operationally simple conditions.

In relation to catalytic applications, a different type of amine-bearing carbon dots was used in combination with CO_2, which was employed to recycle the system [126]. In this case, the CDs used were obtained from citric acid and alkyl diamines including primary, secondary, and tertiary amines bearing short alkyl chain with up to eight carbon atoms. Changes in the amine precursor did not affect the final material in terms of morphology, and all samples displayed a high number of amines, up to c. 4 mmol/g, as evaluated from a combination of XPS and TGA experiments. The carbon dots obtained using 1,4-diaminobutane as an amine precursor were used to promote the Knoevenagel condensation affording 2-(4-bromobenzylidene)malononitrile in 1-octanol. After product filtration, the CDs were recovered by CO_2 bubbling in a biphasic system. This operation led to the transfer of CDs to the aqueous phase, likely as a consequence of carbonate ion formation at the surface of CDs, as revealed by ^{13}C-NMR experiments. This catalyst recycling procedure allowed to use the same batch of CDs to perform the reaction up to six times.

Clearly, additional work remains to be done regarding the exploitation of amino groups as catalytic units supported onto CDs.

8.5 Amines for the Engineering of Hybrid Organic–Inorganic Nanomaterials

The role of amines in the engineering of hybrid organic–inorganic nanomaterials is manifold; these valuable compounds find applications in several stages of nanomaterial development, from the synthesis and functionalization to their practical implementation. Within the context of developing synthetic strategies for organic–inorganic hybrids, amines have been applied to a very broad range of nanosized materials encompassing metal chalcogenide and perovskite quantum dots, noble metal nanoparticles, and metal oxide nanoparticles, including transition or rare-earth metals. Another class of organic–inorganic hybrids for which amines can provide tailored properties is that of SAMs on flat surfaces. Nanomaterial surface functionalization is a relevant feature that controls their interaction with other nanoscale or mesoscale objects and therefore underpins their applications. In this respect, amines and amino groups have been exploited in various manners. Indeed, positively charged nanoparticles or SAMs displaying amino groups on their surface can effectively interact with other polyelectrolytes, either natural or synthetic, by charge complementarity or hydrogen bond formation. Alternatively, surface-accessible amines can be used for developing complex, yet well-defined, higher order systems by, for instance, complexation of metal ions or covalent bond formation.

The reliability, safety, and scalability of the nanomaterial preparation attained by using amines are of outmost importance and have nowadays set a benchmark. Besides, the excellent control over nanomaterial properties allowed by these approaches is witnessed by the large body of literature in this field and the impact on everyday life considering the increasing role of nanotechnology products. This makes an exhaustive description of the amino group chemistry in the context of hybrid organic–inorganic nanomaterial development out of reach. This notwithstanding, some relevant aspects and approaches are quite general and will be presented in Section 8.5.1, with specific reference at SAMs on flat surfaces, semiconductor quantum dots, and metal and metal oxide nanoparticles.

8.5.1 Amines as Head Groups or End Groups on Self-assembled Monolayers on Flat Surfaces

SAMs on flat surfaces are assemblies of small molecules anchored by either chemisorption or physisorption on a substrate. A variety of species can form SAMs, but the most studied are alkanethiols that represent the preferred species for SAMs formation on metal surfaces [127]. SAMs formed by using alkylamines on flat metal surfaces are usually less stable than those formed by thiols.

The amine head groups interact weakly with the metal surfaces (Figure 8.16a) [128], and this is consistent with the mismatch between the relatively hard nature of amines and the soft acid nature of metals in the zero oxidation state. Density functional theory (DFT) calculations pointed out that the interaction energy of amines with gold surfaces is about seven times smaller than the gold–thiol interaction [129]. Therefore, if the latter is about 40 kcal/mol [130], the nitrogen–gold interaction is about 6 kcal/mol, comparable to those of

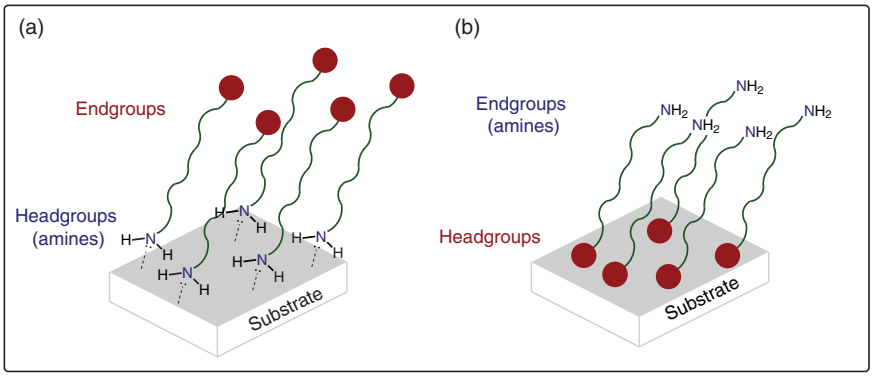

Figure 8.16 Schematic representations of 2D-SAM, (a) amine head groups anchored to the substrate surface and (b) amine end groups exposed to the outer surface of the SAM.

hydrogen bonds. A notable exception is monolayer formation on iron surfaces. In this case, a series of anilines [131] and alkylamines [132] were reported to effectively inhibit surface corrosion by monolayer formation. Most likely, such a strong binding is a consequence of the amino group interacting with iron in the pseudo-fourfold hollow sites of the Fe(110) surface. The adsorption of amines remains weak even on surfaces exposing hydroxyl groups such as mica, quartz, or glass [133]. On such materials, the formation of a monolayer is mainly driven by hydrogen bonding to the substrate and strongly depends on the nature of the solvent used. The obtained SAM is often incomplete and mechanically unstable, as probed by AFM [134]. More frequently, amines are used as capping agents for noble metal nanoparticles and their use in this domain will be analyzed with more detail in Section 8.5.2.

Amino groups are very often introduced on the outer surface of the 2D SAMs (Figure 8.16b), where they serve as reactive moieties for further functionalization or for the formation of adhesive surfaces, e.g. for cells, proteins, and biomolecules [135]. In this context, the amine-terminated SAMs proved to be more efficient than hydroxyl-terminated SAMs and are essentially as active as carboxyl group-terminated SAMs, albeit a large degree of nonspecific adsorption was also pinpointed for the amine-terminated monolayers [135c, 136]. One of the most exploited reactions has been the functionalization of SAMs formed by aminopropylsilane, on Si/SiO_2 or glass. Although 2D SAMs are mainly formed by reaction of surface available hydroxy groups with the aminopropylsilane, SAMs can also be formed by CVD [137]. The reason for the popularity of such a simple SAM has been the possibility to interface it with DNA, either covalently or noncovalently, retaining the hybridization ability of the employed strands [138]. The reliability of multiple noncovalent interactions has allowed their use in the formation of elaborated architectures. As an example, multilayer films containing DNA and polyamines were easily prepared, by simply dipping the substrate into solutions of polyamine and DNA, sequentially [139]. In the resulting multilayer architecture, the change complementarity between protonated amines and deprotonated phosphate groups, together with hydrogen bonding interactions, provided the observed stability. Interestingly, these interactions occurred at the expense of

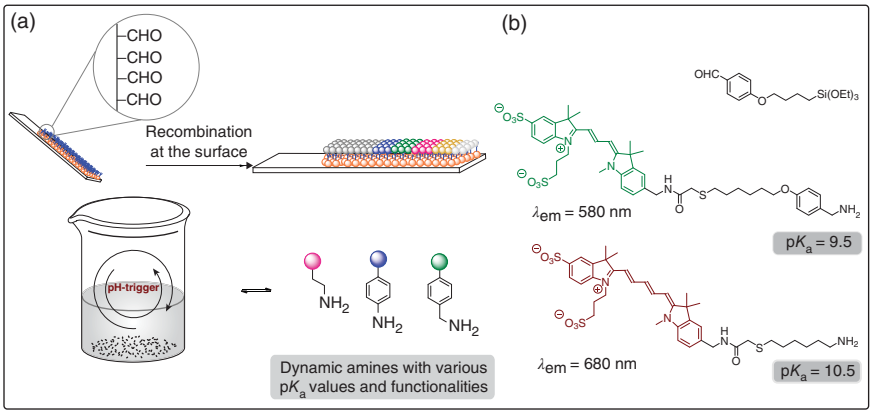

Figure 8.17 Schematic representation of the strategy described in Ref. [147] to prepare surface gradients via imine bond formation. Source: Based on Tauk et al. [147].

hydration of the two charged groups, leading to a weakly hydrated multilayer structure. To complete the overview on noncovalent exploitation of amino groups, the use of polylysine should also be mentioned because it is a prominent polycationic amine-rich polymer, frequently used for surface functionalization [140].

Besides noncovalent strategies, the covalent reactivity of amine-terminated SAMs has been extensively studied and proved to be extremely versatile in the context of SAM functionalization [141]. Covalent functionalization included (i) amide bond formation upon reaction with an activated ester or an acid chloride [142]; (ii) nucleophilic acyl substitutions, e.g. upon reaction with di-(*N*,*N*-succinimidyl) carbonate, which allowed further reaction with the hydroxy group of β-cyclodextrin forming carbamate bonds [143]; or nucleophilic acyl substitutions affording (9-fluorenyl)methoxycarbonyl-protected amines, thus changing the hydrophobicity of the monolayer [144]. The reactivity of amino groups was also exploited in surface-patterning applications, e.g. via microcontact printing or photodeprotection reactions involving amines as reagent or – more frequently – products [145].

One strategy that has proven particularly versatile for the functionalization of surfaces is imine bond formation, which can potentially merge the advantages of covalent chemistry with the benefits originating from its dynamic nature [146]. An elegant example of the versatility of imine formation reactions at surfaces has been presented by Giuseppone and coworkers [147]. In this work, a substrate was covered via silanization with an appropriate aldehyde-terminating unit, and the obtained monolayer was used to prepare surface gradients via imine bond formation. To achieve this target, the monolayer with terminal aldehydes was immersed in a solution containing both aliphatic and benzylic amines, having different pK_a values, thus displaying a different reactivity toward imine formation at a given pH (Figure 8.17). While imine formation was taking place at the surface, the substrate was slowly removed from the solution. Simultaneously, the pH was modified with the addition of triethylamine or trichloroacetic acid.

Under these conditions, as a consequence of amine protonation, the preferential partner for imine formation changed over time inducing the formation of surface gradients. The

solidity of this approach was also demonstrated by implementing this strategy in an organic solvent or for the functionalization with biomolecules.

8.5.2 Alkylamines in the Preparation of Semiconductor Quantum Dots

II–VI semiconductor QDs such as CdSe, CdS, ZnS, ZnSe, etc., are very often prepared under conditions resembling those described in the landmark work by Bawendi and coworkers [148]. These required the use of tri-*n*-octylphosphine (TOP) and tri-*n*-octylphosphine oxide (TOPO) acting both as a solvent system and capping agents. However, TOP and TOPO are far from ideal, suffering the disadvantage of high toxicity. These issues prompted the development of synthetic conditions replacing the need of phosphine species in part or altogether. Long-chain alkylamines can be used in the temperature range, above 250 or 300 °C, required for the synthesis of quantum dots and are safer and more environmentally benign than TOP and TOPO. Indeed, several alkylamines, and especially oleylamine (OLE), are commonly used in the syntheses of these nanomaterials, often in association with fatty acids, high boiling point alkenes, 1-octadecene (ODE) being the most common, and TOP/TOPO mixtures [149].

Although suitable as solvents for high-temperature reactions, long-chain alkylamines are solid at room temperature (Dod has a melting point of 27–28 °C and a boiling point of 250 °C; tetradecylamine has a melting point of 40 °C and a boiling point of 290 °C), which hinders the work-up procedures. Accordingly, among fatty amines, the choice of election for the preparation of quantum dots and other nanomaterials is OLE because at room temperature, it is in the liquid state (melting point 18–26 °C), has a boiling point of 350 °C, and is commercially available, although of technical grade. Besides serving as suitable solvents, alkylamines also act as reagents, mainly in the activation of the chalcogenide precursors and capping agents for the nanocrystals. Activation of metal carboxylate precursors by amines has also been reported in the preparation of ZnSe and ZnS QDs [150].

8.5.2.1 Sulfur–Amine and Selenium–Amine Systems

Although the complex nature of the solutions obtained from elemental sulfur in certain amines is known since 1930 [151], and despite the use of these compounds in the preparation of metal chalcogenide semiconductor NPs is well established, it is only recently that a clear understanding of these systems is emerging. Elemental sulfur dissolves in certain amines to give colored solutions, which were thought to contain *N*,*N*'-polythiobisamines, formed by scission of S—S bonds in the S_8 molecules with evolution of hydrogen sulfide. Electron spin resonance (ESR) studies of these solutions pointed out the presence of sulfur-centered free radicals formed by homolytic scission of the S—S bonds of the *N*,*N*′-polythiobisamines [152]; Raman spectroscopy analyses were in line with this suggestion [153]. More recently 1D-, 2D-, and DOSY NMR analyses of the S_8-octylamine model system pointed out that, at low temperature, S_8-alkylamine solutions contain mainly alkylammonium polysulfides [154], and a small amount of *N*,*N*′-polythiobisamine, which is however sufficient to produce enough hydrogen sulfide necessary to the formation of alkylammonium polysulfides. Under the high-temperature conditions typically used for the nanocrystal preparation, the polysulfide ion reacting with excess amine produces hydrogen sulfide and other by-products, which likely comprise

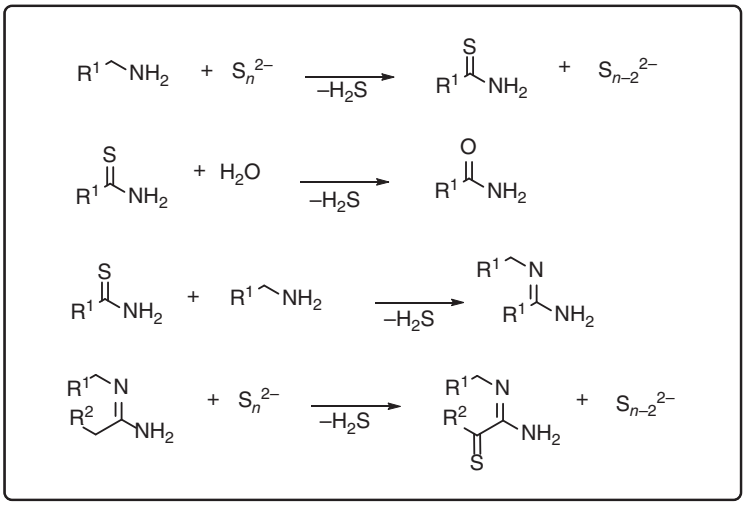

Figure 8.18 Reaction pathways in sulfur–octylamine solution at 130 °C. Source: From Thomson et al. [154].

amides and amidines that arise from a common intermediate identified in octylthioamide. Possibly, α-thioketoamidines are also formed by reaction of amidines with polysulfides. Overall, the authors propose the mechanistic scheme depicted in Figure 8.18 and suggest alkylammonium hydrogen sulfide as the sulfur precursor in the preparation of metal sulfide nanocrystals.

As a compelling demonstration of the importance of thioamide intermediates in the synthesis of quantum dots, the authors report the synthesis of PbS nanocrystals at 25 °C using commercially available thioacetamide dissolved in OLE as a sulfur precursor [154].

In contrast with elemental sulfur, selenium dissolves poorly in neat alkylamines. However, it dissolves at high concentration in the simultaneous presence of OLE and of reducing agents such as sodium borohydride [155], or alkanethiols [156]. In the latter case, the mechanism of dissolution was found to be dependent on the reduction potential of the thiol, and the rate of dissolution on the nature of the amine that is faster in the order primary > secondary > tertiary. Using low molecular weight alkanethiols such as ethanethiol, which could be removed as well as the corresponding disulfide under vacuum, leads to highly concentrated selenium solutions in OLE. In the reaction system made of OLE/ODE/sodium borohydride, elemental selenium can be dissolved in 10 hours at room temperature. Conversely, by replacing the unsaturated OLE with hexylamine, no reaction occurs after 10 hours at 50 °C. Octadecene itself is known to dissolve selenium, but reaction takes place at temperatures exceeding 200 °C [157]. This indicates that the simultaneous presence of an unsaturation and amino group are essential for reaction with selenium at low temperature [158], while at higher temperature, amines are not necessary because in both ODE and saturated alkanes, selenium powder generates the hydrogen selenide or other reactive selenium hydride species involved in the QD nucleation [154, 159].

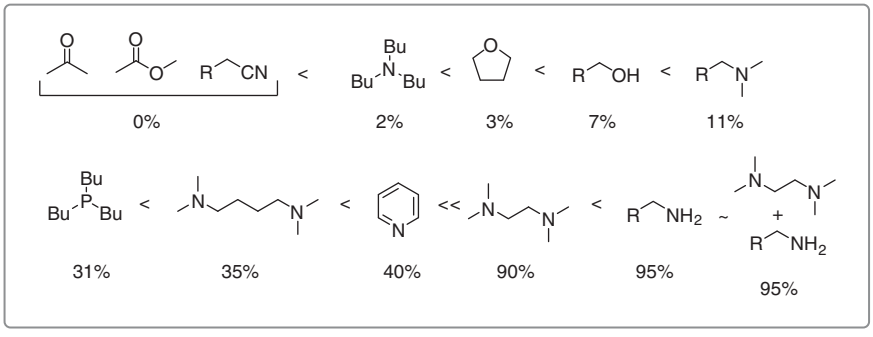

Figure 8.19 Relative displacement potency labeled with the percentage of Lewis base-Cd(carboxylate)$_2$ displaced in a 2.0 M solution of the of Lewis base-type ligand. Source: From Anderson et al. [163].

8.5.2.2 Capping Ligands for Quantum Dots and Ligand Exchange by Amines

Primary alkylamines are able to displace other weak ligands from the surface of quantum dots, in particular, they can readily displace TOPO [160]. However, amines used as a cosurfactant during CdSe clusters or NP synthesis cannot compete with fatty acids for QD passivation if fatty acids are present as in the surfactant mixture [161]. Conversely, if fatty acids are not used in excess, i.e. not used as cosurfactants, the coating by amines dominates even with TOP and TOPO in solution [162]. On the other hand, Owen demonstrated that interaction of tetramethylethylendiamine (TMEDA) or mixtures of primary amines and TMEDA with carboxylate-protected CdSe QD results in the displacement of cadmium carboxylate from cadmium selenide nanocrystals, and not in the displacement of the carboxylate as such [163]. Different Lewis bases exert the same effect albeit to a very different extent (Figure 8.19).

By using TMEDA, the displacement of cadmium carboxylate complexes is nearly quantitative in few minutes and results in a dramatic drop in photoluminescence quantum yield (PLQY). However, samples exposed to solely primary amines display significantly increased PLQY, despite losing a large proportion of surface-bound cadmium carboxylates. Recent works by Peng and coworkers point out that the coordination of fatty acids on CdSe nanocrystals is strongly facet dependent [164], with the polar {100} and {111} facets being involved in chelating and bridging binding modes with the carboxylate ligands. On the other hand, the nonpolar {110} facets are substantially reconstructed with yet very weak coordination bonds to the surface lattice. Considering CdSe nanoplates, Peng and coworkers displayed that exposure to amines maintains the carboxylate ligands on the polar {100} basal planes, while the mostly nonpolar side facets are weakly passivated with amines [165].

Amine ligands are important stabilizers for QD, and among the ligands usually encountered in the passivation of CdSe quantum dots, amines give more dynamic passivation than carboxylates and less than thiols [166]. Therefore, the ease of displacement depends on the relative affinity of the ligands originally present on the nanocrystals surface. Desorption rate constants reported in the literature are variable, ranging from 0.01 to 1.5×10^{-4} s^{-1}.

These values were generally obtained by analysis of the photoluminescence of the QD upon exposure to amines, but an NMR analysis by Hens and coworkers using octylamine- and pyridine-capped CdSe QD gave a significantly lower limit, which sets the desorption rate constant to values higher than $50\,s^{-1}$ [167]. The very same system studied by Peng and coworkers monitoring the photoluminescence increase upon exposure to octylamine gave a desorption rate constant of $0.01\,s^{-1}$ [166].

Because the CdSe pyridine was shown to offer a labile and reversible bonding with the surface cadmium ions, refluxing TOPO-capped CdSe QD in pyridine allows complete removal of the original ligand without altering the structural properties of the QD [168]. The large difference in Lewis basicity between pyridine and primary amines or thiols leads to consider pyridine-treated CdSe nanocrystals essentially "naked" once used in the presence of stronger ligands, such as the above-mentioned amines and thiols.

Displacement of weak ligands such as TOPO from the surface of CdSe QD by alkylamines affords materials with higher PLQY. Mulvaney and coworker displayed that PLQY enhancement by amines decreases in the order primary $\gg$ secondary $>$ tertiary [160]. This enhancement is correlated with the passivation of surface trap states that enable non radiative deactivation of the excited QD reducing PLQY. Fatty amines are electron-donating ligands and should thus passivate Cd sites on the surface [169]. However, the exact nature of these surface trap states is elusive, and only recently, experimental and theoretical work is shedding light on the proper ligands needed to increase the PLQY of semiconductor of different compositions [170].

Polymeric amines also interact with QD. Indeed, polyallylamine has been used to transfer TOPO-capped CdSe QD in water [171], and CdSe/ZnS QDs protected by PAMAM dendrimers, soluble in water, have been proposed as QD for cancer cell targeting [172]. Polyethyleneimine (PEI) has also been used similarly, representing the "handle" for QD functionalization in a copolymer ligand consisting of PEG-grafted PEI reported by Nie and coworker [173].

Because of their high PLQY, semiconductor QDs are interesting alternatives to organic fluorophores for a range of applications in the chemical, biochemical, and biomedical field. All these applications rely on the anchoring to the NP surface suitable moieties to endow the QD with solubility in aqueous media. Amine-functionalized ligands also represent convenient species for the introduction of functional groups on the outer surface of the QD. However, given the dynamic nature of amine passivation, it has to rely on multivalent interaction with the nanocrystals. In this perspective, Parak and coworker demonstrated that the interaction of pyridine-modified amphiphilic polymers can be used to functionalize TOPO-capped QD by displacing part of the native ligands, while establishing hydrophobic interactions between the hydrophobic moieties in the polymer and the remaining TOPO on the QD surface [174].

8.5.3 Alkylamines as Reagents for the Synthesis and Passivation of Metal Nanoparticles

8.5.3.1 Alkylamines as Capping Agents for Metal Nanoparticles

Amines are commonly used in the preparation of noble metal and metal oxide NPs. In this context, amines may act as a cosolvent, reducing agent, and surfactant or may react

with the metal precursor forming the actual species involved in the nanostructure preparation. The amino group anchors on the metal surface while the alkyl chain provides stabilization by Van der Waals interactions and steric hindrance, preventing irreversible particle aggregation. Different kinds of amines have been used in the preparation of metal NPs, acting according to one or more of the above-mentioned roles. These range from simple long-chain alkylamines and dialkylamines to 4-(dimethylamino)pyridine (DMAP) and amino-functionalized dendrimers [175]. In addition, the availability of chiral enantiopure amines, either synthetic or from the chiral pool, enables the development of NPs, which may be used for enantioselective catalysis [176].

Amines have been reported to promote the formation of gold and platinum NPs from Au(III) or Pt(II) precursors, without the need of any additional reducing agent [177]. In other cases, the reactions are carried out in the presence of stronger reducing agents such as borane–amine complexes or sodium borohydride [175d, 178]. Usually, the particles obtained by using amines as the capping agent can be recovered by precipitation from the reaction mixture and centrifugation. In addition, amines can be completely removed, if necessary, leaving "naked" particles by treatment with acetic acid and/or heating [179].

Among amines, OLE is, very often, the choice of election [180]. Nearly monodisperse amine-capped Ag and Au NPs in the 6–21-nm (Au) and 8–32-nm (Ag) size ranges and polydispersites below 7% could be prepared in large scale by refluxing hydrogen tetrachloroaurate or silver acetate and OLE in toluene for 120 minutes. The metal NP sizes can be tuned by varying the concentrations of the metal precursor and of the amine. The surfactant concentration has only a small influence on NPs size, but it influences polydispersity, which can be reduced below 10% when, for example, at least 65 equiv of the amine with respect to the gold precursor are used [181]. Xia and coworkers reported the preparation of silver multiply twinned particles by reaction of silver trifluoroacetate in *o*-dichlorobenzene in the presence of OLE at 180 °C [182]. Upon reaction of these silver NPs with hydrogen tetrachloroaurate, and excess OLE, galvanic replacement of silver takes place with the formation of hollow particles. The extra OLE was found to be critical for the formation of well-defined, uniform hollow structures free of AgCl contamination because of the formation of a soluble complex between AgCl and OLE during the replacement reaction.

Complexation of AuCl and AuBr with OLE makes possible to prepare Au NPs by thermolysis under mild conditions (60 °C in $CHCl_3$) without using an additional reducing agent [183]. In this procedure, particles with 12.7 nm diameter and size distribution of 8% could be obtained and the authors suggest a putative reaction mechanism involving the formation of dioleylamine as a by-product. Besides its role in Au(I) complexation, OLE acts as surface stabilizer and the authors point out that in the presence of octadecylamine instead of OLE, the particles displayed an average diameter of 100 nm, a clear evidence that even though the *Z*-configuration of OLE double bond does not play a role in the synthesis, the steric requirements of the OLE backbone strongly drive the formation of smaller NPs. The use of OLE as a surfactant and aminoborane complexes as reducing agents has been studied as a convenient method for the fine-tuning of NPs size from 2 to about 7 nm, using a mixture of OLE/octane 1/1 and by running the reaction at different temperatures [184].

Similar results were achieved using OLE and tetralin as a solvent (Figure 8.20) [178b]. The critical role of straight chain alkane solvents in the polydispersity of these materials in these syntheses was pointed out by Zheng and coworkers [185].

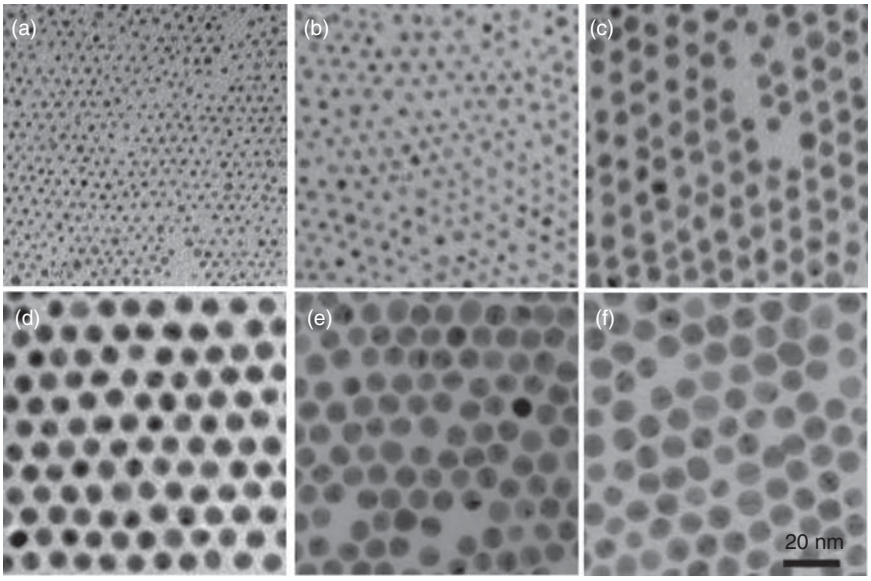

Figure 8.20 Representative TEM images for oleylamine-based synthesis of gold NPs run at temperatures. (a) 40 °C, (b) 35 °C, (c) 25 °C, (d) 15 °C, (e) 10 °C, and (f) 2 °C. Source: Reproduced from Peng et al. [178b]. Copyright 2008, Springer.

In association with fatty acids, amines have provided a way to produce anisotropic nanostructures. OLE has been used for the preparation of gold nanowires starting from AuCl as a precursor. In this case, the amine forms a complex with AuCl and these complexes interact among themselves via aurophilic interactions spontaneously forming extended 1D superstructures that upon reduction give the ultrathin nanowires [186]. Xing reported a method for preparing ultrathin single-crystalline gold nanowires in solution using $HAuCl_4$, OLE as a surfactant, and triisopropylsilane (TIPS) as a reducing agent, the reaction being complete within a few hours at room temperature [187]. Strongly anisotropic nanocrystals of transition metals and rare-earth oxide are obtained by using oleic acid and OLE in octadecene [188]. OLE, in association with oleic acid, has been used as a stabilizer for FePt NPs [179] and Pt nanocubes [189] where the surfactant mixture also served for shape control. Concave Pt nanocrystals with high-index {411} facets (Figure 8.21) were prepared solvothermally by reduction of hexachloroplatinic acid using poly(vinylpyrrolidone) (PVP) as the surfactant in the presence of methylamine [190]. Tuning of the concavity could be achieved by changing the amount of methylamine used in the synthesis.

After the pioneering work by Crooks and coworkers [191], dendrimers containing amino groups have been widely used as templates for the preparation of encapsulated metal NPs using sodium borohydride as a reducing agent in these syntheses [192]. Amino dendrimers are particularly effective because they are able to preconcentrate metal ions by complexation and a wide range of metal NPs has been prepared by this method, including Cu, Au, Pt, Pd, and Ru NPs. In these systems, the limited stabilization provided by the amine moiety is reinforced by the multiple contacts provided by the dendrimeric structure. Dendrimeric

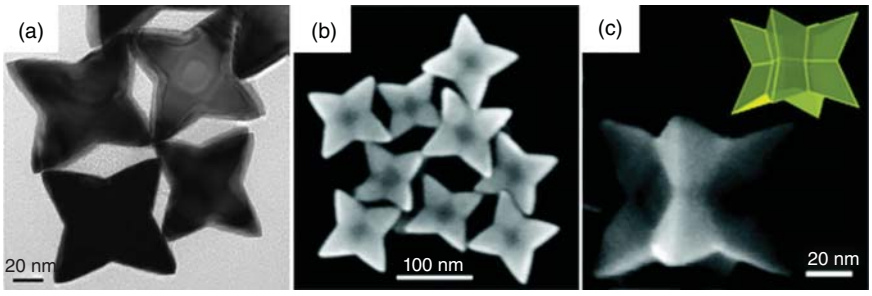

Figure 8.21 (a) TEM images of the concave Pt nanocrystals. (b) SEM image of the as-prepared concave Pt nanocrystals. (c) High-magnification SEM image of a single concave Pt nanocrystal. The top-right inset shows an ideal geometrical model of the concave Pt nanocrystal with the same orientation as the nanocrystal in the SEM image. Source: Reproduced with permission from Huang et al. [190]. Copyright 2011, American Chemical Society.

amines grafted on solid supports or NPs can also serve for the syntheses of metal NPs, which results in an assembled composite material [193].

8.5.3.2 Displacement of Amines from the Surface of Metal Nanoparticles

Qualitatively, metals in the zero oxidation state behave as soft acids and will interact strongly with soft bases, it is therefore reasonable that a hard base such as an amine will interact with metal particles only weakly and in a reversible manner. Indeed, gold NPs protected by amines have been considered to be kinetically stable instead of thermodynamically stable [194]. Therefore, metal NPs prepared in the presence of amines are amenable of an easy ligand displacement reaction with ligands that bind more strongly to the metal surfaces. The weakly absorbed OLE on gold NPs can be readily displaced with aliphatic thiols by adding a toluene solution of the OLE-capped gold NPs to a boiling solution of 5–10 equiv (based on gold) of the thiol in the same solvent [181]. OLE-capped metal NPs have been used in exchange reactions with different thiols giving essentially clean substitution products. This procedure was found to be effective even using binary blends of thiols, which give rise to NP displaying in the monolayer the same composition of the feeding mixture [184]. On the other hand, exchange of OLE by octadecanethiol has been reported to be incomplete on batches of NPs containing excess amine surfactant even after prolonged time and repeated exchanges in the presence of excess thiol [195].

8.5.4 Amines on the Outer Surface of Organic–inorganic Hybrid Nanoparticles

Introduction of amino groups at the outer nanoparticle surface can be used to provide hybrid NP systems with specific ways to interact with other nanosized objects or a reactive handle for further functionalization. To this end, bifunctional ligands are required. One functional moiety binds the metal NP surface while a distal amino group is displayed on the outer surface of the nanoparticle. Typically, for transition metal oxide or silica NPs, these bifunctional ligands are aminosilanes such as (aminopropyl)-triethoxysilane (APTS) [196], while for noble metal NPs or semiconductor quantum dots, the preferred ligands are

ω-aminoalkanethiols. In the case of iron oxide NPs, a cathecolate ligand such as dopamine has also been used, which was also reported to increase the colloidal stability of these systems [197]. However, the silane chemistry can also be used to introduce amino groups on the surface of gold NPs and QD by first functionalizing the metal surface with silane thiol, such as 3-mercaptopropyltrimethoxysilane (MPS), and afterward reacting the alkoxysilane groups with aminosilanes [198].

Alternatively, NPs can be coated with polycationic polymers, either natural or synthetic, such as chitosan [199], polyallylamine, or PEI [200]. In this case, the polymers provide both stabilization and reactive groups that can be used for further functionalization. For this approach to be effective, the surface of the metal particles has to be negatively charged or protected by labile ligands. In some cases, negative charge on the particle surface may come from the synthesis such as in the case of colloidal gold prepared by using the citrate reduction method [201]. Alternatively, a negatively charged surface can be obtained by exposing the particles to negatively charged polymers to form a first layer, which is covered afterward by an amine-functionalized polymer. Lennox and coworkers displayed the viability of this approach by reporting a series of Au/DMAP/anionic polymer/cationic polymer systems [202] and, with little variation, this strategy is still largely pursued. Quantification of reactive amino groups accessible on the surface of gold NPs is possible by labeling the amino groups with suitable reporter moieties, used for conventional amine assay, that can be quantified after disruption of the nanostructure [8]. Instead, quantification of the total number of amino groups on the nanostructure surface can be achieved by assessing the amount of amine containing ligands left behind in the solution after incubation with the Aunanostructures [8].

The large majority of applications of these nanosystems concerns biomedical applications. Indeed, the protonated amines on the outer NP surface can interact with negatively charged biomolecules, thanks to charge complementarity or hydrogen bonding, such as proteins [203] or nucleic acids [204]. In this latter context, amine-functionalized nanostructures and the related nanostructures decorated with ammonium ions can be efficiently used for gene transfection, or drug delivery [205], or to target the bacterial cell wall [206]. Amine derived from lysine or dendronized lysine have been introduced on the outer surface of NPs, providing a way to modulate the ability of the nanoparticle system to condense DNA and to deliver this cargo to cells [207]. The same approach has been applied to the delivery of small-interfering ribonucleic acid (siRNA) either by using metal NPs [208] or polymeric core–shell NPs [209].

Polyallylamine and its derivatives are often used as polymeric coating in passivating the nanoparticle surface but also to provide surface-accessible amino groups. Very often, successive layers of polymers with opposite charges are used. This is also a strategy to endow particles with improved gene delivery properties by reducing the synthetic efforts to a minimum. In this respect, gold NPs stabilized by chitosan, coated with a layer of charge-reversible poly(allylamine hydrochloride)-citraconic anhydride, and PEI could be loaded with siRNA protecting the payload against enzymatic degradation and displaying excellent transfection properties (Figure 8.22) [210]. PEI can also be used in the same way for siRNA delivery [211].

Besides gold NPs, which are interesting because of their low toxicity, other materials such as silica have been used to develop amine-functionalized scaffolds that can be loaded with nucleic acids for gene delivery [212]. Amine-functionalized hollow mesoporous silica NPs

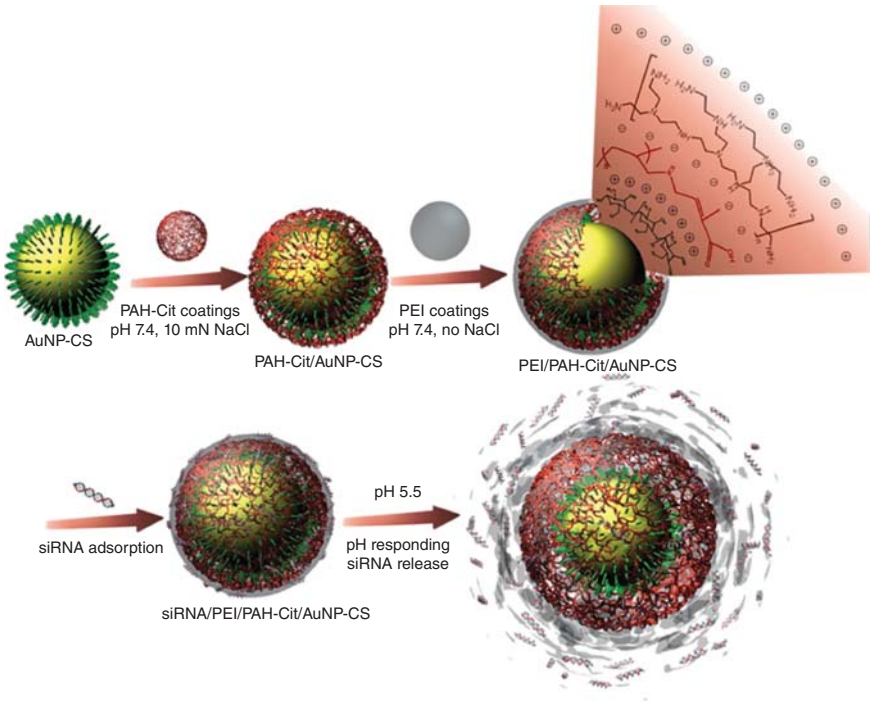

Figure 8.22 Assembly steps for siRNA/PEI/PAH-Cit/AuNP–CS complexes and pH-responsive release of siRNA. Source: Reproduced with permission from Han et al. [210]. Copyright 2011, American Chemical Society.

could be efficiently used as vectors for drug delivery with high efficiency, thanks to their large amine surface giving enhanced interactions with cells [213].

The advantage of these systems is the relatively easy introduction of amino groups on silica surface by using readily available aminosilanes. Nevertheless, more engineered particles such as polylysine-functionalized mesostructured silica were also proposed for gene delivery [214]. The extent of surface coverage in amino-functionalized silica has also an impact on the toxicity of this material [215]. Although these applications rely on electrostatic interactions between a positively charged nanoparticle surface and negatively charged biopolymers or biosystems, surface available amines can be exploited as ligands for the complexation of transition metal ions. Indeed, macrocyclic secondary amines such as triazacyclononane or chelating amines have been extensively used to anchor metal ions on the outer surface of gold NPs. Some of these constructs display remarkable catalytic activity in hydrolytic processes [216]. However, NPs decorated with macrocyclic, chelating, and ligands have found application in the complexation of metal ions such as Gd(III) that have a relevant role in diagnostic techniques based on magnetic resonance imaging [217].

The ability of amine-functionalized NPs to complex metal ions has also an impact on water detoxification. In this respect, by associating the magnetic properties of iron oxide NPs with surface-exposed amines, it has been possible to devise systems capable of capturing toxic metal cations from wastewater or contaminated solutions with the benefit of an easy recovery by applying magnetic fields [218]. The same concept has been proposed for the magnetic capture of bacterial pathogens [219].

Ligands on the surface of metal NPs can be designed to include short-peptide sequences displaying amino groups from lysine or histidine residues. These constructs were originally developed to mimic natural enzymes, and indeed, NPs functionalized with peptides containing histidine display catalytic activity in the hydrolysis of active esters with cooperative mechanisms and substrate recognition [220]. The imidazole moiety has also been exploited in the development of nanoparticles-based multivalent exo-receptors for porphyrin arrays [221]. Peptides have been studied as suitable surface capping agents for gold NPs, identifying the minimal requirement, in terms of sequence length and sequence composition to endow the particles with high stability [222]. Peptides have also been applied as coating molecules on silica-based nanomaterials, where lysine-rich sequences have been exploited to boost cell penetration and drug delivery properties [223]. This strategy is also useful when lysine-rich peptides have therapeutic properties themselves [224].

Amino groups at the outer surface of NPs can also be covalently coupled with other species by standard amide bond formation with reactive esters [225]. Nanoparticles for this kind of applications are commercially available from many suppliers. Amino groups can be reacted with activated linkers to further enlarge the variety of surface-reactive groups such as maleimide units suitable for click chemistry reactions [226].

Amino groups on the surface of NPs can also be used to covalently link NPs among themselves, or NPs with polymers carrying carboxylic groups spatially localized along the backbone, forming well-defined arrays [227]. Covalent conjugation with proteins is also possible [228]. Bawendi and coworkers displayed the viability of this strategy reporting an early compelling example of biocompatible QD for cellular imaging [229]. In this system, the protecting layer was engineered by using heterobifunctional ligands incorporating dihydrolipoic acid for anchoring to the nanocrystal, a short PEG spacer for solubility purposes, and an amine or carboxylate end group for further functionalization.

8.5.5 Postfunctionalization of Amine-Terminated Organic–Inorganic Hybrid Nanoparticles

Amine-functionalized surfaces have been exploited to set up approaches in which a solid support carrying amino groups is used for the immobilization of NPs. Immobilization relies on either charge complementarity between the particles and the support or the affinity of metal surfaces for amine ligands. Given the reversible nature of the binding between amines and metal surfaces, the immobilization can be temporary or permanent. In the case of temporary immobilization, this strategy can be used to mask part of the NP surface while the exposed surface can be conveniently functionalized. Overall, this process yields Janus particles. Shumaker-Parry demonstrated the viability of this strategy by immobilizing citrate-capped Au-NPs on amine-functionalized glass slides and replacing the exposed citrate ligands with α,ω-hydroxyundecanethiol. Removal of the particles from the glass slide by sonication and their treatment with amine- or acid-terminated thiols gave two sets of Janus Au-NPs with hydroxyl/amine and hydroxyl/acid functional hemispheres. Coupling of these particles with amide bond formation gave rise to nanoparticle dimers in high yield [230]. On similar lines, amine-functionalized Janus gold NPs were prepared by grafting gold NPs on silica particles coated with a ligand comprising an imine moiety. After functionalization

of the exposed second half of the nanoparticle surface, hydrolysis of the imine released the Janus particles in solution [231].

Permanent immobilization on amine-functionalized solid support is also possible, and this approach has been used to anchor NPs for the preparation of composite materials and catalysts, which display improved performance with respect to model system. Indeed, amine-functionalized zeolites, obtained by using 3-aminopropyltrimethoxysilane, were found to bind Pd and Pt NPs giving materials useful in hydrogenation and Heck reactions [232], and Pd NPs anchored on amino group-terminated SiO_2 were proposed as highly effective catalysts in the model reduction of 4-nitrophenol [233]. Pd NPs supported on amino-functionalized silica was reported as a catalyst for the reduction of Cr(VI) [234]. Nitrogen-rich polymers have also been used to entrap Pd NPs, and the system has been tested in model processes for biofuel upgrading [235]. Citrate-capped gold NPs could also be anchored to poly(allylamine hydrochloride)-modified polymer poly(glycidyl) methacrylate submicrospheres to yield raspberry-like composites with catalytic activity in the reduction of 4-nitrophenol [236].

DMAP-functionalized gold NPs could be grafted, with ligand displacement, on the surface of amine-functionalized boron nitride nanotubes as nanoscale templates for assembly and integration with other nanoscale materials [237]. Nanoparticle assembly on carbon nanostructures gives rise to an important class of composites materials for which amine functionalization can provide strong interaction and coupling [238]. Indeed, amino silica layers formed on the surface of CNTs has been used for the assembly of gold NPs on the surface obtaining materials useful as electrocatalysts for oxygen reduction [239]. Accelerated catalytic activity of Pd NPs in the hydrogenation of quinoline was observed upon supporting these materials on amine-rich silica hollow nanospheres [240].

References

1 Sun, Y., Kunc, F., Balhara, V. et al. (2019). *Nanoscale Advances* 1: 1598–1607.

2 (a) Troll, W. and Cannan, R.K. (1953). *The Journal of Biological Chemistry* 200: 803–811. (b) Kaiser, E., Colescott, R.L., Bossinger, C.D., and Cook, P.I. (1970). *Analytical Biochemistry* 34: 595–598. (c) Sarin, V.K., Kent, S.B.H., Tam, J.P., and Merrifield, R.B. (1981). *Analytical Biochemistry* 117: 147–157.

3 Kunc, F., Balhara, V., Brinkmann, A. et al. (2018). *Analytical Chemistry* 90: 13322–13330.

4 Zhao, L., Baccile, N., Gross, S. et al. (2010). *Carbon* 48 (13): 3778–3787.

5 Baer, D.R., Engelhard, M.H., Johnson, G.E. et al. (2013). *Journal of Vacuum Science and Technology A* 31 (5): 050820.

6 Kralj, S., Drofenik, M., and Makovec, D. (2011). *Journal of Nanoparticle Research* 13: 2829–2841.

7 (a) Ederer, J., Janoš, P., Ecorchard, P. et al. (2017). *RSC Advances* 7: 12464–12473. (b) Chen, Y. and Zhang, Y. (2011). *Analytical and Bioanalytical Chemistry* 399: 2503–2509.

8 (a) Battigelli, A., Wang, J.T.-W., Russier, J. et al. (2013). *Small* 9 (21): 3610–3619. (b) Ménard-Moyon, C., Fabbro, C., Prato, M., and Bianco, A. (2011). *Chemistry* 17

(11): 3222–3227. (c) Xia, X., Yang, M., Wang, Y. et al. (2012). *ACS Nano* 6 (1): 512–522. (d) Jarre, G., Heyer, S., Memmel, E. et al. (2014). *Beilstein Journal of Organic Chemistry* 10: 2729–2737. (e) Poli, E., Chaleix, V., Damia, C. et al. (2014). *Analytical Methods* 6: 9622–9627. (f) Quintana, M., Spyrou, K., Grzelczak, M. et al. (2010). *ACS Nano* 4 (6): 3527–3533.

9 Kroto, H.W., Heath, J.R., O'Brien, S.C. et al. (1985). *Nature* 318: 162–164.

10 Krätschmer, W., Lamb, L.D., Fostiropoulos, K., and Huffman, D.R. (1990). *Nature* 347: 354–358.

11 Iijima, S. (1991). *Nature* 354: 56–58.

12 Novoselov, K.S., Geim, A.K., Morozov, S.V. et al. (2004). *Science* 306: 666–669.

13 (a) Martin, N. and Bodwell, G. (2019). *Accounts of Chemical Research* 52: 2757–2759. (b) Delgado, J.L., Ángeles Herranza, M., and Martín, N. (2008). *Journal of Materials Chemistry* 18: 1417–1426.

14 (a) Hirsch, A. (1998). *Topics in Current Chemistry* 199: 1–65. (b) Chen, Z., Thiel, W., and Hirsch, A. (2003). *ChemPhysChem* 1: 93–97. (c) Quintana, M., Vázquez, E., and Prato, M. (2013). *Accounts of Chemical Research* 46: 138–148.

15 Lin, T., Zhang, W.D., Huang, J., and He, C. (2005). *The Journal of Physical Chemistry. B* 109: 13755–13760.

16 Jiang, D., Sumpter, B.G., and Dai, S. (2007). *The Journal of Chemical Physics* 126: 134701–134706.

17 Maggini, M., Scorrano, G., and Prato, M. (1993). *Journal of the American Chemical Society* 115: 9798–9799.

18 Bahr, J.L., Yang, J., Kosynkin, D.V. et al. (2001). *Journal of the American Chemical Society* 123: 6536–6542.

19 Georgakilas, V., Kordatos, K., Prato, M. et al. (2002). *Journal of the American Chemical Society* 124: 760–761.

20 Hashimoto, T. and Maruoka, K. (2015). *Chemical Reviews* 115: 5366–5412.

21 (a) Prato, M. and Maggini, M. (1998). *Accounts of Chemical Research* 31 (9): 519–526. (b) Kordatos, K., Da Ros, T., Bosi, S. et al. (2001). *The Journal of Organic Chemistry* 66: 4915–4920.

22 Maggini, M. and Menna, E. (2002). *Fullerenes: From Synthesis to Optoelectronic Properties*, Chapter 1 (eds. D.M. Guldi and N. Martin), 1–50. Dordrech: Kluwer Academic Publishers.

23 Martín, N., Altable, M., Filippone, S. et al. (2006). *Angewandte Chemie, International Edition* 45: 110–114.

24 Filippone, S., Maroto, E.E., Martín-Domenech, A. et al. (2009). *Nature Chemistry* 1: 578–582.

25 (a) Maroto, E.E., de Cózar, A., Filippone, S. et al. (2011). *Angewandte Chemie, International Edition* 50: 6060–6064. (b) Sawai, K., Takano, Y., Izquierdo, M. et al. (2011). *Journal of the American Chemical Society* 133: 17746–17752. (c) Maroto, E.E., Filippone, S., Martín-Domenech, A. et al. (2012). *Journal of the American Chemical Society* 134: 12936–12938. (d) Marco-Martínez, J., Marcos, V., Reboredo, S. et al. (2013). *Angewandte Chemie, International Edition* 52: 5115–5119. (e) Marco-Martínez, J., Reboredo, S., Izquierdo, M. et al. (2014). *Journal of the American Chemical Society* 136: 2897–2904.

26 Fernández-García, J.M., Evans, P.J., Filippone, S. et al. (2019). *Accounts of Chemical Research* 52: 1565–1574.
27 Ménard-Moyon, C., Izard, N., Doris, E., and Mioskowski, C. (2006). *Journal of the American Chemical Society* 128: 6552–6553.
28 Harris, P.J.F. (2001). *Carbon Nanotubes and Related Structures: New Materials for the Twenty-First Century*. Cambridge: Cambridge University Press.
29 Nikolaev, P., Bronikowski, M.J., Bradley, R.K. et al. (1999). *Chemical Physics Letters* 313: 91–97.
30 Tasis, D., Tagmatarchis, N., Bianco, A., and Prato, M. (2006). *Chemical Reviews* 106: 1105–1136.
31 (a) Pantarotto, D., Partidos, C.D., Graff, R. et al. (2003). *Journal of the American Chemical Society* 125: 6160–6164. (b) Pantarotto, D., Singh, R., McCarthy, D. et al. (2004). *Angewandte Chemie, International Edition* 43: 5242–5246. (c) Bianco, A., Hoebeke, J., Godefroy, S. et al. (2005). *Journal of the American Chemical Society* 127: 58–59. (d) Singh, R., Pantarotto, D., McCarthy, D. et al. (2005). *Journal of the American Chemical Society* 127: 4388–4396. (e) Wu, W., Wieckowski, S., Pastorin, G. et al. (2005). *Angewandte Chemie, International Edition* 44: 6358–6362.
32 Toma, F.M., Sartorel, A., Iurlo, M. et al. (2010). *Nature Chemistry* 2: 826–831.
33 (a) Bianco, A. and Prato, M. (2003). *Advanced Materials* 15: 1765–1768. (b) Bianco, A. (2004). *Expert Opinion on Drug Delivery* 1: 57–65. (c) Bianco, A., Kostarelos, K., Partidos, C.D., and Prato, M. (2005). *Chemical Communications*: 571–577.
34 (a) Prato, M., Kostarelos, K., and Bianco, A. (2008). *Accounts of Chemical Research* 41: 60–68. (b) Kostarelos, K., Bianco, A., and Prato, M. (2009). *Nature Nanotechnology* 4: 627–633.
35 Herrero, M.A., Toma, F.M., Al-Jamal, K.T. et al. (2009). *Journal of the American Chemical Society* 131: 9843–9848.
36 Sartorel, A., Carraro, M., Scorrano, G. et al. (2008). *Journal of the American Chemical Society* 130: 5006–5007.
37 (a) Lee, K.M., Li, L., and Dai, L. (2005). *Journal of the American Chemical Society* 127: 4122–4123. (b) Stephenson, J.J., Hudson, J.L., Leonard, A.D. et al. (2007). *Chemistry of Materials* 19: 3491–3498.
38 Lipinsk, M.E., Rebelo, S.L.H., Pereira, M.F.R. et al. (2012). *Carbon* 50: 3280–3294.
39 Brunetti, F.G., Herrero, M.A., Muñoz, J.d.M. et al. (2008). *Journal of the American Chemical Society* 130: 8094–8100.
40 Brunetti, F.G., Herrero, M.A., Muñoz, J.d.M. et al. (2007). *Journal of the American Chemical Society* 129: 14580–14581.
41 (a) Geim, A.K. and Novoselov, K.S. (2007). *Nature Materials* 6: 183–191. (b) Chen, L., Hernandez, Y., Feng, X., and Müllen, K. (2012). *Angewandte Chemie, International Edition* 51: 7640–7654.
42 Wick, P., Louw-Gaume, A.E., Kucki, M. et al. (2014). *Angewandte Chemie, International Edition* 53: 7714–7718.
43 (a) Geim, A.K. (2009). *Science* 324: 1530–1534. (b) Castro Neto, A.H., Guinea, F., Peres, N.M.R. et al. (2009). *Reviews of Modern Physics* 81: 109–162. (c) Balandin, A. (2011). *Nature Materials* 10: 569–581.

44 (a) Sheng Su, D., Perathoner, S., and Centi, G. (2013). *Chemical Reviews* 113: 5782–5816. (b) Wu, S., He, Q., Tan, C. et al. (2013). *Small* 9: 1160–1172. (c) Bonaccorso, F., Sun, Z., Hasan, T., and Ferrari, A.C. (2010). *Nature Photonics* 4: 611–622. (d) Pumera, M. (2011). *Energy & Environmental Science* 4: 668–674.
45 Criado, A., Melchionna, M., Marchesan, S., and Prato, M. (2015). *Angewandte Chemie, International Edition* 54: 10734–10750.
46 Wang, Q.H., Jin, Z., Kim, K.K. et al. (2012). *Nature Chemistry* 4: 724–732.
47 Hernandez, Y., Nicolosi, V., Lotya, M. et al. (2008). *Nature Nanotechnology* 3: 563–568.
48 Hossain, Z., Walsh, M.A., and Hersam, M.C. (2010). *Journal of the American Chemical Society* 132: 15399–15403.
49 Fan, X., Nouchi, R., and Tanigaki, K. (2011). *Journal of Physical Chemistry C* 115: 12960–12964.
50 (a) Montellano, A., Da Ros, T., Bianco, A., and Prato, M. (2011). *Nanoscale* 3: 4035–4041. (b) Schinazi, R.F., Sijbesma, R., Srdanov, G. et al. (1993). *Antimicrobial Agents and Chemotherapy* 37: 1707–1710. (c) Ikeda, A., Hatano, T., Kawaguchi, M. et al. (1999). *Chemical Communications*: 1403–1404.
51 Richardson, C.F., Schuster, D.I., and Wilson, S.R. (2000). *Organic Letters* 2: 1011–1014.
52 Shao, L., Bai, Y., Huang, X. et al. (2009). *Chemical Physics* 116: 323–326.
53 Singh, S.K., Singh, M.K., Kulkarni, P.P. et al. (2012). *ACS Nano* 6: 2731–2740.
54 Biglova, Y.N. and Mustafin, A.G. (2019). *RSC Advances* 9: 22428–22498.
55 Nakamura, T., Ishihara, M., Ohana, T. et al. (2004). *Chemical Communications*: 1336–1337.
56 Singh, M.K., Titus, E., Gonçalves, G. et al. (2010). *Nanoscale* 2: 700–708.
57 Jiang, Z., Jiang, Z.J., Tian, X., and Chen, W. (2014). *Journal of Materials Chemistry A* 2: 441–450.
58 (a) Guo, S.J. and Dong, S.J. (2011). *Chemical Society Reviews* 40: 2644–2672. (b) Ferrari, A.C. et al. (2015). *Nanoscale* 7: 4598–4810.
59 Ciesielski, A. and Samorì, P. (2014). *Chemical Society Reviews* 43: 381–398.
60 Parviz, D., Irin, F., Shah, S.A. et al. (2016). *Advanced Materials* 28: 8796–8818.
61 Vázquez, E., Giacalone, F., and Prato, M. (2014). *Chemical Society Reviews* 43: 58–69.
62 León, V., Quintana, M., Herrero, M.A. et al. (2011). *Chemical Communications* 47: 10936–10938.
63 Backes, C., Hauke, F., and Hirsch, A. (2011). *Advanced Materials* 23: 2588–2601.
64 Iijima, S., Yudasaka, M., Yamada, R. et al. (1999). *Chemical Physics Letters* 309: 165–170.
65 Harris, P.J.F., Tsang, S.C., Claridge, J.B., and Green, M.L.H. (1994). *Journal of the Chemical Society, Faraday Transactions* 90: 2799–2802.
66 Azami, T., Kasuya, D., Yuge, R. et al. (2008). *Journal of Physical Chemistry C* 112 (5): 1330–1334.
67 (a) Murata, K., Kaneko, K., Kokai, F. et al. (2000). *Chemical Physics Letters* 331 (1): 14–20. (b) Zhu, S. and Xu, G. (2010). *Nanoscale* 2: 2538–2549. (c) Ajima, K., Yudasaka, M., Murakami, T. et al. (2005). *Molecular Pharmaceutics* 2 (6): 475–480.
68 Deng, S.Y., Lei, J.P., Huang, Y. et al. (2012). *Chemical Communications* 48: 9159–9161.
69 Cioffi, C., Campidelli, S., Sooambar, C. et al. (2007). *Journal of the American Chemical Society* 129: 3938–3945.

70 Vizuete, M., Gomez-Escalonilla, M.J., Fierro, J.L.G. et al. (2014). *Chemical Science* 5: 2072–2080.
71 Isobe, H., Tanaka, T., Maeda, R. et al. (2006). *Angewandte Chemie, International Edition* 45: 6676–6680.
72 (a) Nakamura, E., Koshino, M., Tanaka, T. et al. (2008). *Journal of the American Chemical Society* 130: 7808–7809. (b) Lacotte, L., Garcia, A., Decossas, M. et al. (2008). *Advanced Materials* 20: 2421–2426.
73 Miyako, E., Russier, J., Mauro, M. et al. (2014). *Angewandte Chemie, International Edition* 53: 13121–13125.
74 Tagmatarchis, N., Maigne, A., Yudasaka, M., and Iijima, S. (2006). *Small* 2: 490–494.
75 Lucío, M.I., Opri, R., Pinto, M. et al. (2017). *Journal of Materials Chemistry B* 5: 8821–8832.
76 Pagona, G., Karousis, N., and Tagmatarchis, N. (2008). *Carbon* 46: 604–610.
77 Cioffi, C., Campidelli, S., Brunetti, F.G. et al. (2006). *Chemical Communications*: 2129–2131.
78 Karfa, P., De, S., Majhi, K. et al. (2019). Functionalization of carbon nanostructures. In: *Comprehensive Nanoscience and Nanotechnology*, 2e, vol. 2, 123–144.
79 Valey, T.S., Hirani, M., Harrison, G., and Holt, K.B. (2014). *Faraday Discussions* 172: 349.
80 Popov, V.A., Egorovn, A.V., Savilov, S.V. et al. (2013). *Journal of Surface Investigation: X-Ray, Synchrotron and Neutron Techniques* 7: 1034–1043.
81 Liu, Y., Gu, Z., Margrave, J.L., and Khabashesku, V.N. (2004). *Chemistry of Materials* 16: 3924–3930.
82 Mochalin, V.N., Neitzel, I., Etzold, B.J.M. et al. (2011). *ACS Nano* 5 (9): 7494–7502.
83 Krüger, A., Liang, Y., Jarre, G., and Stegk, J. (2006). *Journal of Materials Chemistry* 16: 2322–2328.
84 (a) Yu, Y., Yang, X., Liu, M. et al. (2019). *Nanoscale Adv.* 1: 3406–3412; (b) Yu, Y., Nishikawa, M., Liu, M. et al. (2018). *Nanoscale* 10: 8969–8978.
85 Ugarte, D. (1992). *Nature* 359: 707–709.
86 Plonska-Brzezinska, M.E. (2019). *Chemistry of Nanomaterials* 5: 568–580.
87 Georgakilas, V., Guldi, D.M., Signorini, R. et al. (2003). *Journal of the American Chemical Society* 125: 14268–14269.
88 Cioffi, C.T., Palkar, A., Melin, F. et al. (2009). *Chemistry - A European Journal* 15: 4419–4427.
89 Huang, W., Fernando, S., Allard, L.F., and Sun, Y.-P. (2003). *Nano Letters* 3: 565–568.
90 Rettenbacher, A.S., Elliott, B., Hudson, J.S. et al. (2006). *Chemistry - A European Journal* 12: 376–387.
91 Wei-De, Z. and Wen-Hui, Z. (2009). *Journal of Sensors* 2009: 160698.
92 Tran, T.H., Lee, J.-W., Lee, K. et al. (2008). *Sensors and Actuators B: Chemical* 129: 67–71.
93 Zeng, Y.-L., Huang, Y.-F., Jiang, J.-H. et al. (2007). *Electrochemistry Communications* 9 (1): 185–190.
94 (a) Schedin, F., Geim, A., Morozov, S. et al. (2007). *Nature Materials* 6: 652. (b) Wehling, T., Novoselov, K., Morozov, S. et al. (2008). *Nano Letters* 8: 173–177.

95 Tung, T.T., Nine, M.J., Krebsz, M. et al. (2017). *Advanced Functional Materials* 27: 1702891–1702947.
96 Tang, X., Mager, N., Vanhorenbeke, B. et al. (2017). *Nanotechnology* 28: 1–11.
97 (a) Baker, S.N. and Baker, G.A. (2010). *Angewandte Chemie, International Edition* 49: 6726–6744. (b) Georgakilas, V., Perman, J.A., Tucek, J., and Zboril, R. (2015). *Chemical Reviews* 115: 4744–4822. c Lim, S.Y., Shen, W., and Gao, Z. (2015). *Chemical Society Reviews* 44: 362–381.
98 Xu, X., Ray, R., Gu, Y. et al. (2004). *Journal of the American Chemical Society* 126: 12736–12737.
99 (a) Roy, P., Chen, P.-C., Periasamy, A.P. et al. (2015). *Materials Today* 18: 447–458. (b) Sun, Y.-P., Zhou, B., Lin, Y. et al. (2006). *Journal of the American Chemical Society* 128: 7756–7757. (c) Hutton, G.A.M., Martindale, B.C.M., and Reisner, E. (2017). *Chemical Society Reviews* 46: 6111–6123. (d) Li, H., Kang, Z., Liu, Y., and Lee, S.-T. (2012). *Journal of Materials Chemistry* 22: 24230–24253.
100 Arcudi, F., Đorđević, L., and Prato, M. (2019). *Accounts of Chemical Research* 52 (8): 2070–2079.
101 (a) Hu, Y., Yang, J., Tian, J., and Yu, J.-S. (2015). *Journal of Materials Chemistry B* 3 (27): 5608–5614. (b) Shi, Q.-Q., Li, Y.-H., Xu, Y. et al. (2014). *RSC Advances* 4 (4): 1563–1566. (c) Krysmann, M.J., Kelarakis, A., Dallas, P., and Giannelis, E.P. (2012). *Journal of the American Chemical Society* 134 (2): 747–750.
102 See e.g. Verma, N.C., Yadav, A., and Nandi, C.K. (2019). *Nature Communications* 10: 2391.
103 (a) Schneider, J., Reckmeier, C.J., Xiong, Y. et al. (2017). *Journal of Physical Chemistry C* 121: 2014–2022. (b) Li, D., Jing, P., Sun, L. et al. (2018). *Advanced Materials* 30: 1705913.
104 Fang, Q., Dong, Y., Chen, Y. et al. (2017). *Carbon* 118: 319–326.
105 Song, Y., Zhu, S., Zhang, S. et al. (2015). *Journal of Materials Chemistry C* 3: 5976–5984.
106 Righetto, M., Privitera, A., Fortunati, I. et al. (2017). *Journal of Physical Chemistry Letters* 8: 2236–2242.
107 Essner, J.B., Kist, J.A., Polo-Parada, L., and Baker, G.A. (2018). *Chemistry of Materials* 30 (6): 1878–1887.
108 (a) Jiang, J., He, Y., Li, S., and Cui, H. (2012). *Chemical Communications* 48: 9634–9636. (b) Martindale, B.C.M., Hutton, G.A.M., Caputo, C.A. et al. (2017). *Angewandte Chemie, International Edition* 56: 6459–6463. (c) Mazzier, D., Favaro, M., Agnoli, S. et al. (2014). *Chemical Communications* 50: 6592–6595. (d) Choi, Y., Thongsai, N., Chae, A. et al. (2017). *Journal of Industrial and Engineering Chemistry* 47: 329–335. (e) Li, F., Li, Y., Yang, X. et al. (2018). *Angewandte Chemie, International Edition* 130 (9): 2401–2406.
109 (a) Strauss, V., Margraf, J.T., Dolle, C. et al. (2014). *Journal of the American Chemical Society* 136 (49): 17308–17316. (b) Sciortino, A., Cannizzo, A., and Messina, F. (2018). *Carbon* 4: 67.
110 (a) Tong, G., Wang, J., Wang, R. et al. (2015). *Journal of Materials Chemistry B* 3: 700–706. (b) Konstantinos, D. (2016). *Current Organic Chemistry* 20 (6): 682–695.

111 Manioudakis, J., Victoria, F., Thompson, C.A. et al. (2019). *Journal of Materials Chemistry C* 7: 853–862.
112 (a) Liu, C., Zhang, P., Zhai, X. et al. (2012). *Biomaterials* 33 (13): 3604–3613. (b) Hu, L., Sun, Y., Li, S. et al. (2014). *Carbon* 67: 508–513. (c) Dou, Q., Fang, X., Jiang, S. et al. (2015). *RSC Advances* 5: 46817–46822. (d) Pierrat, P., Wang, R., Kereselidze, D. et al. (2015). *Biomaterials* 51: 290–302.
113 (a) Arcudi, F., Đorđević, L., and Prato, M. (2016). *Angewandte Chemie, International Edition* 55: 2107–2112. (b) Đorđević, L., Arcudi, F., and Prato, M. (2019). *Nature Protocols* 14: 2931–2953.
114 Carrara, S., Arcudi, F., Prato, M., and De Cola, L. (2017). *Angewandte Chemie, International Edition* 56: 4757–4761.
115 Arcudi, F., Đorđević, L., and Prato, M. (2017). *Angewandte Chemie, International Edition* 56: 4170–4173.
116 Rigodanza, F., Đorđević, L., Arcudi, F., and Prato, M. (2018). *Angewandte Chemie, International Edition* 57: 5062–5067.
117 Đorđević, L., Arcudi, F., D'Urso, A. et al. (2018). *Nature Communications* 9: 3442.
118 Liu, W., Li, C., Ren, Y. et al. (2016). *Journal of Materials Chemistry B* 4: 5772–5788.
119 Arcudi, F., Strauss, V., Đorđević, L. et al. (2017). *Angewandte Chemie, International Edition* 56: 12097–12101.
120 D'Souza, F. and Ito, O. (2009). *Chemical Communications*: 4913–4928.
121 (a) Zheng, M., Liu, S., Li, J. et al. (2014). *Advanced Materials* 26 (21): 3554–3560. (b) Gomez, I.J., Arnaiz, B., Cacioppo, M. et al. (2018). *Journal of Materials Chemistry B* 6: 5540–5548.
122 (a) Bertelsen, S. and Jørgensen, K.A. (2009). *Chemical Communications*: 2178–2189. (b) Melchiorre, P., Marigo, M., Carlone, A., and Bartoli, G. (2008). *Angewandte Chemie, International Edition* 47: 6138–6171. (c) Melchiorre, P. (2012). *Angewandte Chemie, International Edition* 51: 9748–9770. (d) Lelais, G. and MacMillan, D.W.C. (2006). *Aldrichimica Acta* 39: 79–87. (e) Nielsen, M., Worgull, D., Zweifel, T. et al. (2011). *Chemical Communications* 47: 632–649. (f) List, B. (2006). *Chemical Communications*: 819–824. (g) Seebach, D., Groselj, U., Badine, D.M. et al. (2008). *Helvetica Chimica Acta* 91: 1999–2034. (h) Seebach, D., Gilmour, R., Groselj, U. et al. (2010). *Helvetica Chimica Acta* 93: 603–634. (i) Schmid, M.B., Zeitler, K., and Gschwind, R.M. (2010). *Angewandte Chemie, International Edition* 49: 4997–5003. (j) Schmid, M.B., Zeitler, K., and Gschwind, R.M. (2011). *Chemical Science* 2: 1793–1803.
123 van der Helm, M.P., Klemm, B., and Eelkema, R. (2019). *Nature Reviews Chemistry* 3: 491–508.
124 Testa, C., Zammataro, A., Pappalardo, A., and Trusso Sfrazzetto, G. (2019). *RSC Advances* 9: 27659–27664.
125 Rosso, C., Filippini, G., and Prato, M. (2019). *Chemistry - A European Journal* 25: 16032–16036.
126 Pei, X., Xiong, D., Wang, H. et al. (2018). *Angewandte Chemie, International Edition* 57: 3687–3691.
127 Love, J.C., Estroff, L.A., Kriebel, J.K. et al. (2005). *Chemical Reviews* 105: 1103–1170.
128 de la Llave, E., Clarenc, R., Schiffrin, D.J., and Williams, F.J. (2014). *Journal of Physical Chemistry C* 118: 468–475.

129 Hoft, R.C., Ford, M.J., McDonagh, A.M., and Cortie, M.B. (2007). *Journal of Physical Chemistry C* 111: 13886–13891.
130 Ulman, A. (1996). *Chemical Reviews* 96: 1533–1554.
131 (a) Jeyaprabha, C., Sathiyanarayanan, S., and Venkatachari, G. (2005). *Applied Surface Science* 246: 108. (b) Khaled, K.F. and Hackerman, N. (2003). *Materials Chemistry and Physics* 82: 949–960.
132 Feng, Y., Chen, S., You, J., and Guo, W. (2007). *Electrochimica Acta* 53: 1743–1753.
133 Pujari, S.P., Scheres, L., Marcelis, A.T.M., and Zuilhof, H. (2014). *Angewandte Chemie, International Edition* 53: 6322–6356.
134 Bentez, J.J., Kopta, S., Ogletree, D.F., and Salmeron, M. (2002). *Langmuir* 18: 6096–6100.
135 (a) Faucheux, N., Schweiss, R., Lützow, K. et al. (2004). *Biomaterials* 25: 2721–2730. (b) Arima, Y. and Iwata, H. (2007). *Journal of Materials Chemistry* 17: 4079–4087. (c) Arima, Y. and Iwata, H. (2015). *Acta Biomaterialia* 26: 72–81. (d) Hasan, A., Pattanayek, S.K., and Pandey, L.M. (2018). *ACS Biomaterials Science & Engineering* 4: 3224–3233.
136 Leea, M.H., Brass, D.A., Morris, R. et al. (2005). *Biomaterials* 26: 1721–1730.
137 (a) Feng Zhang, F., Sautter, K., Larsen, A.M. et al. (2010). *Langmuir* 26: 14648–14654. (b) Yadav, A.R., Sriram, R., Carter, J.A., and Miller, B.L. (2014). *Materials Science and Engineering: C* 35: 283–290.
138 (a) Chriseyl, L.A., Lee, G.U., and O'Ferrall, C.E. (1996). *Nucleic Acids Research* 24 (15): 3031–3039. (b) Caviani-Pease, A., Solas, D., Sullivan, E.J. et al. (1994). *Proceedings of the National Academy of Sciences of the United States of America* 91: 5022–5026.
139 Sukhorukov, G.B., Montrel, M.M., Petrov, A.I. et al. (1996). *Biosensors & Bioelectronics* 11 (9): 913–922.
140 (a) Jordon, C.E., Frey, B.L., Kornguth, S., and Corn, R.M. (1994). *Langmuir* 10 (10): 3642–3648. (b) Frey, B.L. and Corn, R.M. (1996). *Analytical Chemistry* 68 (18): 3187–3193. (c) Ruiz-Taylor, L.A., Martin, T.L., Zaugg, F.G. et al. (2001). *Proceedings of the National Academy of Sciences of the United States of America* 98 (3): 852–857.
141 (a)Chechik, V., Crooks, R.M., and Stirling, C.J.M. (2000). *Advanced Materials* 12: 1161–1171. (b) Sullivan, T.P. and Huck, W.T.S. (2003). *European Journal of Organic Chemistry*: 17–29.
142 Fox, M.A., Whitesell, J.K., and McKerrow, A.J. (1998). *Langmuir* 14: 816–820.
143 Campiña, J.M., Martins, A., and Silva, F. (2009). *Electrochimica Acta* 55: 90–103.
144 Frutos, A.G., Brockman, J.M., and Corn, R.M. (2000). *Langmuir* 16: 2192–2197.
145 (a) Han, S.W., Lee, I., and Kim, K. (2002). *Langmuir* 18: 182–187. (b) Alonso, J.M., Reichel, A., Piehler, J., and del Campo, A. (2008). *Langmuir* 24: 448–457. (c) Whitesell, J.K. and Chang, H.K. (1993). *Science* 261: 73–76. (d) Kratzmuller, T., Appelhans, D., and Braun, H.G. (1999). *Advanced Materials* 11 (7): 555–558.
146 (a) Moon, J.H., Shin, W.J., Kim, S.Y., and Park, J.W. (1996). *Langmuir* 12: 4621–4624. (b) Jiang, D., Tang, J., Liu, B. et al. (2003). *Biosensors & Bioelectronics* 18: 1183–1191.
147 Tauk, L., Schröder, A.P., Decher, G., and Giuseppone, N. (2009). *Nature Chemistry* 1: 649–656.
148 Murray, C.B., Norris, D.J., and Bawendi, M.G. (1993). *Journal of the American Chemical Society* 115: 8706–8715.

149 Talapin, D.V., Rogach, A.L., Kornowski, A. et al. (2001). *Nano Letters* 1: 207–211.
150 Li, L.S., Pradhan, N., Wang, Y., and Peng, X. (2004). *Nano Letters* 4: 2261–2264.
151 (a) Levi, T.G. (1930). *Gazzetta Chimica Italiana* 60: 975–987. (b) Levi, T.G. (1931). *Gazzetta Chimica Italiana* 61: 286–293.
152 Hodgson, W.G., Buckler, S.A., and Peters, G.J. (1963). *Journal of the American Chemical Society* 85: 543–546.
153 Sullivan, P.D. (1973). *The Journal of Physical Chemistry* 77: 1859–1861.
154 Thomson, J.W., Nagashima, K., Macdonald, P.M., and Ozin, G.A. (2011). *Journal of the American Chemical Society* 133: 5036–5041.
155 (a) Riha, S., Parkinson, B.A., and Prieto, A.L. (2011). *Journal of the American Chemical Society* 133: 15272–15275. (b) Wang, W., Geng, Y., Yan, P. et al. (1999). *Journal of the American Chemical Society* 121: 4062–4063. (c) Wei, Y., Yang, J., Lin, A.W.H., and Ying, J.Y. (2010). *Chemistry of Materials* 22: 5672–5677.
156 (a) Liu, Y., Yao, D., Shen, L. et al. (2012). *Journal of the American Chemical Society* 134: 7207–7210. (b) Walker, B.C. and Agrawal, R. (2014). *Chemical Communications* 50: 8331–8334.
157 Bullen, C., van Embden, J., Jasieniak, J. et al. (2010). *Chemistry of Materials* 22: 4135–4143.
158 Zimdars, J. and Bredol, M. (2016). *New Journal of Chemistry* 40: 1137–1142.
159 Deng, Z., Cao, L., Tang, F., and Zou, B. (2005). *The Journal of Physical Chemistry. B* 109: 16671–16675.
160 (a) Bullen, C. and Mulvaney, P. (2006). *Langmuir* 22: 3007–3013. (b) Green, M. (2010). *Journal of Materials Chemistry* 20: 5797–5809.
161 Fisher, A.A.E., Osborne, M.A., Day, I.J., and Lucena Alcalde, G. (2019). *Communications Chemistry* 2: 63.
162 Cooper, J.K., Franco, A.M., Gul, S. et al. (2011). *Langmuir* 27: 8486–8493.
163 Anderson, N.C., Hendricks, M.P., Choi, J.J., and Owen, J.S. (2013). *Journal of the American Chemical Society* 135: 18536–18548.
164 Zhang, J., Zhang, H., Cao, W. et al. (2019). *Journal of the American Chemical Society* 141: 15675–15683.
165 Zhu, C., Chen, D., Cao, W. et al. (2019). *Angewandte Chemie, International Edition* 58: 17764–17770.
166 Ji, X., Copenhaver, D., Sichmeller, C., and Peng, X. (2008). *Journal of the American Chemical Society* 130: 5726–5735.
167 Hassinen, A., Moreels, I., de Mello Donegá, C. et al. (2010). *Journal of Physical Chemistry Letters* 1: 2577–2581.
168 Peng, X., Schlamp, M.C., Kadavanich, A.V., and Alivisatos, A.P. (1997). *Journal of the American Chemical Society* 119: 7019–7029.
169 (a) Gao, Y. and Peng, X. (2015). *Journal of the American Chemical Society* 137: 4230–4235. (b) Pu, C. and Peng, X. (2016). *Journal of the American Chemical Society* 138: 8134–8142.
170 (a) Kirkwood, N., Monchen, J.O.V., Crisp, R.W. et al. (2018). *Journal of the American Chemical Society* 140: 15712–15723. (b) du Fossé, I., ten Brinck, S., Infante, I., and Houtepen, A.J. (2019). *Chemistry of Materials* 31: 4575–4583.
171 Zhang, T., Ge, J., Hu, Y., and Yin, Y. (2007). *Nano Letters* 7: 3203–3207.

172 Akin, M., Bongartz, R., Walter, J.G. et al. (2012). *Journal of Materials Chemistry* 22: 11529–11536.
173 Duan, H. and Nie, S. (2007). *Journal of the American Chemical Society* 129: 3333–3338.
174 Carrillo-Carrion, C. and Parak, W.J. (2016). *Journal of Colloid and Interface Science* 478: 88–96.
175 (a) Gandubert, V.J. and Lennox, R.B. (2005). *Langmuir* 21: 6532–6539. (b) Rucareanu, S., Gandubert, V.J., and Lennox, R.B. (2006). *Chemistry of Materials* 18: 4674–4680. (c) Kumar, A., Mandal, S., Selvakannan, P.R. et al. (2003). *Langmuir* 19: 15, 6277–6282. (d) Metin, Ö., Sun, X., and Sun, S. (2013). *Nanoscale* 5: 910–912. (e) Crooks, R.M., Zhao, M., Sun, L. et al. (2001). *Accounts of Chemical Research* 34: 181–190.
176 Zaera, F. (2017). *Chemical Society Reviews* 46: 7374–7398.
177 (a) Liu, X., Atwater, M., Jinhai, W. et al. (2007). *Journal of Nanoscience and Nanotechnology* 7: 3126–3133. (b) Wang, C., Yongjie Hu, Y., Lieber, C.M., and Sun, S. (2008). *Journal of the American Chemical Society* 130: 8902–8903. (c) Wang, C., Hou, Y., Kim, J., and Sun, S. (2007). *Angewandte Chemie, International Edition* 46: 6333–6335. (d) Liu, X., Atwater, M., Wang, J., and Huo, Q. (2007). *Colloids and Surfaces, B: Biointerfaces* 58: 3–7.
178 (a) Mazumder, V. and Sun, S. (2009). *Journal of the American Chemical Society* 131: 4588–4589. (b) Peng, S., Lee, Y., Wang, C. et al. (2008). *Nano Research* 1: 229–234. (c) Manea, F., Bindoli, C., Polizzi, S. et al. (2008). *Langmuir* 24: 4120–4124.
179 Sun, S., Murray, C.B., Weller, D. et al. (2000). *Science* 287: 1989–1992.
180 Mourdikoudis, S. and Liz-Marzán, L.M. (2013). *Chemistry of Materials* 25: 1465–1476.
181 Hiramatsu, H. and Osterloh, F.E. (2004). *Chemistry of Materials* 13: 2509–2511.
182 Lu, X., Tuan, H.-Y., Chen, J. et al. (2007). *Journal of the American Chemical Society* 129: 1733–1742.
183 Lu, X., Tuan, H.-Y., Korgel, B.A., and Xia, Y. (2008). *Chemistry - A European Journal* 14: 1584–1591.
184 Yang, Y., Serrano, L.A., and Guldin, S. (2018). *Langmuir* 34: 6820–6826.
185 Wu, B.-H., Yang, H.-Y., Huang, H.-Q. et al. (2013). *Chinese Chemical Letters* 24: 457–462.
186 Lu, X., Yavuz, M.S., Tuan, H.-Y. et al. (2008). *Journal of the American Chemical Society* 130: 8900–8901.
187 Feng, H., Yang, Y., You, Y. et al. (1984-1986). *Chemical Communications* 2009.
188 Huo, Z., Tsung, C.-K., Huang, W. et al. (2009). *Nano Letters* 9: 1260–1264.
189 Wang, C., Daimon, H., Lee, Y. et al. (2007). *Journal of the American Chemical Society* 129: 6974–6975.
190 Huang, X., Zhao, Z., Fan, J. et al. (2011). *Journal of the American Chemical Society* 133: 4718–4721.
191 Zhao, M., Sun, L., and Crooks, R.M. (1998). *Journal of the American Chemical Society* 120: 4877–4878.
192 (a) Esumi, K., Suzuki, A., Yamahira, A., and Torigoe, K. (2000). *Langmuir* 16: 2604–2608. (b) Pan, C., Pelzer, K., Philippot, K. et al. (2001). *Journal of the American Chemical Society* 123: 7584–7593.
193 (a) Sun, L. and Crooks, R.M. (2002). *Langmuir* 18: 8231–8236. (b) Dhiman, M., Chalke, B., and Polshettiwar, V. (2015). *ACS Sustainable Chemistry & Engineering* 3: 3224–3230.

194 Leff, D.V., Brandt, L., and Heath, J.R. (1996). *Langmuir* 12: 4723–4730.
195 Kluenker, M., Mondeshki, M., Tahir, M.N., and Tremel, W. (2018). *Langmuir* 34: 1700–1710.
196 (a) Bruce, I.J. and Sen, T. (2005). *Langmuir* 21: 7029–7035. (b) Bagwe, R.P., Hilliard, L.R., and Tan, W. (2006). *Langmuir* 22: 4357–4362.
197 Ye, Q., Zhou, F., and Liu, W. (2011). *Chemical Society Reviews* 40: 4244–4258.
198 Jana, N.R., Earhart, C., and Ying, J.Y. (2007). *Chemistry of Materials* 19: 5074–5082.
199 Ferreira, H., Martins, A., Alves da Silva, M.L. et al. (2018). *Journal of Materials Chemistry B* 6: 2104–2115.
200 Zheng, Z., Saar, J., Zhi, B. et al. (2018). *Langmuir* 34: 4614–4625.
201 (a) Turkevich, J., Stevenson, P.C., and Hillier, P. (1953). *The Journal of Physical Chemistry* 57: 670–673. (b) Frens, G. (1973). *Nature Physical Science* 241: 20–22. (c) Kimling, J., Maier, M., Okenve, B. et al. (2006). *The Journal of Physical Chemistry. B* 110: 15700–15707.
202 Dorris, A., Rucareanu, S., Reven, L. et al. (2008). *Langmuir* 24: 2532–2538.
203 Fleischer, C.C. and Payne, C.K. (2014). *Accounts of Chemical Research* 47: 2651–2659.
204 Ghosh, P., Han, G., De, M. et al. (2008). *Advanced Drug Delivery Reviews* 60: 1307–1315.
205 (a) Tiwari, P.M., Vig, K., Dennis, V.A., and Singh, S.R. (2011). *Nanomaterials* 1: 31–63. (b) Daraee, H., Eatemadi, A., Abbasi, E. et al. (2016). *Artificial Cells, Nanomedicine, and Biotechnology* 44: 410–422. (c) Giljohann, D.A., Seferos, D.S., Daniel, W.L. et al. (2010). *Angewandte Chemie, International Edition* 49: 3280–3294. (d) Yang, X., Yang, M., Pang, B. et al. (2015). *Chemical Reviews* 115: 10410–10488. (e) Sandhu, K.K., McIntosh, C.M., Simard, J.M. et al. (2002). *Bioconjugate Chemistry* 13: 3–6.
206 (a) Scaletti, F., Hardie, J., Lee, Y.-W. et al. (2018). *Chemical Society Reviews* 47: 3421–3432. (b) Chen, J., Andler, S.M., Goddard, J.M. et al. (2017). *Chemical Society Reviews* 46: 1272–1283.
207 Ghosh, P.S., Kim, C.-K., Han, G. et al. (2008). *ACS Nano* 2: 2213–2218.
208 Lee, S.H., Bae, K.H., Kim, S.H. et al. (2008). *International Journal of Pharmaceutics* 364: 94–101.
209 Siegwart, D.J., Whitehead, K.A., Nuhn, L. et al. (2011). *Proceedings of the National Academy of Sciences of the United States of America* 108: 12996–13001.
210 Han, L., Zhao, J., Zhang, X. et al. (2012). *ACS Nano* 6: 7340–7351.
211 Lee, Y., Lee, S.H., Kim, J.S. et al. (2011). *Journal of Controlled Release* 155: 3–10.
212 (a) Zelikin, A.N., Becker, A.L., Johnston, A.P.R. et al. (2007). *ACS Nano* 1: 63–69. (b) Chang, J.H., Mou, K.Y., and Mou, C.Y. (2019). *Scientific Reports* 9: 11457.
213 Hao, N., Jayawardana, K.W., Chen, X., and Yan, M. (2015). *ACS Applied Materials & Interfaces* 7: 1040–1045.
214 Hartono, S.B., Gu, W., Kleitz, F. et al. (2012). *ACS Nano* 6: 2104–2117.
215 Hsiao, I.L., Fritsch-Decker, S., Leidner, A. et al. (2019). *Small* 15: 1805400.
216 (a) Bonomi, R., Selvestrel, F., Lombardo, V. et al. (2008). *Journal of the American Chemical Society* 130: 15744–15745. b Bonomi, R., Scrimin, P., and Mancin, F. (2010). *Organic & Biomolecular Chemistry* 8: 2622–2626. (c) Manea, F., Bodar Houillon, F., Pasquato, L., and Scrimin, P. (2004). *Angewandte Chemie, International Edition* 43: 6165–6169.

217 (a) Kreyling, W.G., Abdelmonem, A.M., Ali, Z. et al. (2015). *Nature Nanotechnology* 10: 619–623. (b) Nicholls, F.J., Rotz, M.W., Ghuman, H. et al. (2016). *Biomaterials* 77: 291–306. (c) Song, Y., Xu, X., MacRenaris, K.W. et al. (2009). *Angewandte Chemie, International Edition* 48: 9143–9147. (d) Moriggi, L., Cannizzo, C., Dumas, E. et al. (2009). *Journal of the American Chemical Society* 131: 10828–10829. (e) Şologan, M., Padelli, F., Giachetti, I. et al. (2019). *Nanomaterials* 9: 879. (f) Rotz, M.W., Culver, K.S.B., Parigi, G. et al. (2015). *ACS Nano* 9: 3385–3396.
218 Hao, Y.M., Man, C., and Hu, Z.B. (2010). *Journal of Hazardous Materials* 184: 392–399.
219 Huang, Y.-F., Wang, Y.-F., and Yan, X.-P. (2010). *Environmental Science & Technology* 44: 7908–7913.
220 (a) Pengo, P., Baltzer, L., Pasquato, L., and Scrimin, P. (2007). *Angewandte Chemie (International Ed. in English)* 46: 400–404. (b) Pengo, P., Polizzi, S., Pasquato, L., and Scrimin, P. (2005). *Journal of the American Chemical Society* 127: 1616–1617. (c) Pengo, P., Broxterman, Q.B., Kaptein, B. et al. (2003). *Langmuir* 19: 2521–2524.
221 Fantuzzi, G., Pengo, P., Gomila, R. et al. (2003). *Chemical Communications*: 1004–1005.
222 Christopher Doty, R., Hussain, I., Nichols, R.J. et al. (2004). *Journal of the American Chemical Society* 126: 10076–10084.
223 (a) Zhang, D., Wang, J., and Xua, D. (2016). *Journal of Controlled Release* 229: 130–139. (b) Hu, J.-J., Xiao, D., and Zhang, X.-Z. (2016). *Small* 12: 3344–3359.
224 Luo, G.-F., Chen, W.-H., Liu, Y. et al. (2014). *Scientific Reports* 4: 6064.
225 (a) Mikhaylova, M., Kim, D.K., Berry, C.C. et al. (2004). *Chemistry of Materials* 16: 2344–2354. (b) Gu, Y.J., Cheng, J., Lin, C.C. et al. (2009). *Toxicology and Applied Pharmacology* 237: 196–204.
226 Hristov, D.R., Rocks, L., Kelly, P.M. et al. (2015). *Scientific Reports* 5: 17040.
227 Sardar, R. and Shumaker-Parry, J.S. (2008). *ACS Nano* 8: 731–736.
228 Clarke, S., Pinaud, F., Beutel, O. et al. (2012). *ACS Nano* 6: 11080–11087.
229 Liu, W., Howarth, M., Greytak, A.B. et al. (2008). *Journal of the American Chemical Society* 130: 1274–1284.
230 Sardar, R., Heap, T.B., and Shumaker-Parry, J.S. (2007). *Journal of the American Chemical Society* 129: 5356–5357.
231 Wu, S., Tan, S.-Y., Ang, C.Y. et al. (2015). *Chemical Communications* 51: 11622–11625.
232 Mandal, S., Roy, D., Chaudhari, R.V., and Sastry, M. (2004). *Chemistry of Materials* 16: 3714–3724.
233 Liu, J., Hao, J., Hu, C. et al. (2018). *Journal of Physical Chemistry C* 122: 2696–2703.
234 Celebi, M., Yurderi, M., Bulut, A. et al. (2016). *Applied Catalysis, B: Environmental* 180: 53–64.
235 Singuru, R., Dhanalaxmi, K., Shit, S.C. et al. (2017). *ChemCatChem* 9: 2550–2564.
236 Li, M. and Chen, G. (2013). *Nanoscale* 5: 11919–11192.
237 Sainsbury, T., Ikuno, T., Okawa, D. et al. (2007). *Journal of Physical Chemistry C* 111: 12992–12999.
238 Georgakilas, V., Gournis, D., Tzitzios, V. et al. (2007). *Journal of Materials Chemistry* 17: 2679–2694.
239 Guo, S., Dong, S., and Wang, E. (2008). *Journal of Physical Chemistry C* 112: 2389–2393.
240 Guo, M., Li, C., and Yang, Q. (2017). *Catalysis Science & Technology* 7: 2221–2227.